ISSN 1949-8454 (online)

World Journal of *Biological Chemistry*

World J Biol Chem 2022 January 27; 13(1): 1-34

Published by Baishideng Publishing Group Inc

WJBC

World Journal of Biological Chemistry

Contents

Bimonthly Volume 13 Number 1 January 27, 2022

MINIREVIEWS

ORIGINAL ARTICLE

Basic Study

World Journal of Biological Chemistry

Bimonthly Volume 13 Number 1 January 27, 2022

Contents

ABOUT COVER

Editorial Board Member of *World Journal of Biological Chemistry*, Jean Demarquoy, PhD, Professor, Department of Physiology, Université de Bourgogne, UMR PAM université de Bourgogne/Agrosup Dijon, 21000 Dijon, France. jean.demarquoy@u-bourgogne.fr

AIMS AND SCOPE

The primary aim of the *World Journal of Biological Chemistry* (*WJBC*, *World J Biol Chem*) is to provide scholars and readers from various fields of biological chemistry a platform to publish high-quality basic and clinical research articles and communicate their research findings online.

WJBC mainly publishes articles reporting research results and findings obtained in the field of biological chemistry and covering a wide range of topics including bioenergetics, cell biology, chromosomes, developmental biology, DNA, enzymology, extracellular matrices, gene regulation, genomics, glycobiology, immunology, lipids, membrane biology, metabolism, molecular bases of disease, molecular biophysics, neurobiology, plant biology, protein structure and folding, protein synthesis and degradation, proteomics, and signal transduction.

INDEXING/ABSTRACTING

The *WJBC* is now abstracted and indexed in PubMed, PubMed Central, China National Knowledge Infrastructure (CNKI), China Science and Technology Journal Database (CSTJ), and Superstar Journals Database.

RESPONSIBLE EDITORS FOR THIS ISSUE

NAME OF JOURNAL
World Journal of Biological Chemistry

ISSN
ISSN 1949-8454 (online)

LAUNCH DATE
July 26, 2010

FREQUENCY
Bimonthly

PUBLICATION DATE
January 27, 2022

World Journal of Biological Chemistry

Submit a Manuscript: https://www.f6publishing.com

World J Biol Chem 2022 January 27; 13(1): 1-14

DOI: 10.4331/wjbc.v13.i1.1

ISSN 1949-8454 (online)

MINIREVIEWS

Current understanding of the role of tyrosine kinase 2 signaling in immune responses

Ryuta Muromoto, Kenji Oritani, Tadashi Matsuda

ORCID number: Ryuta Muromoto 0000-0002-7474-493X; Kenji Oritani 0000-0002-5571-2457; Tadashi Matsuda 0000-0002-3089-3757.

Author contributions: Muromoto R, Oritani K and Matsuda T participated sufficiently in this work of drafting the article and/or revising the article for the important rational content; all authors gave final approval of the version to be submitted.

Conflict-of-interest statement: Authors declare no conflict of interests for this article.

Supported by Grant-in-Aid for scientific research from Ministry of Education, Culture, Sports, Science and Technology of Japan, No. 19H03364 and No. 20K07010.

Country/Territory of origin: Japan

Specialty type: Immunology

Provenance and peer review: Invited article; Externally peer reviewed.

Peer-review model: Single blind

Peer-review report's scientific quality classification

Grade A (Excellent): 0
Grade B (Very good): 0
Grade C (Good): C
Grade D (Fair): 0

Ryuta Muromoto, Tadashi Matsuda, Department of Immunology, Graduate School of Pharmaceutical Sciences, Hokkaido University, Sapporo 060-0812, Japan

Kenji Oritani, Department of Hematology, International University of Health and Welfare, Narita 286-8686, Japan

Corresponding author: Tadashi Matsuda, PhD, Professor, Department of Immunology, Graduate School of Pharmaceutical Sciences, Hokkaido University, Kita-ku Kita12 Nishi 6, Sapporo 060-0812, Japan. tmatsuda@pharm.hokudai.ac.jp

Abstract

Immune system is a complex network that clears pathogens, toxic substrates, and cancer cells. Distinguishing self-antigens from non-self-antigens is critical for the immune cell-mediated response against foreign antigens. The innate immune system elicits an early-phase response to various stimuli, whereas the adaptive immune response is tailored to previously encountered antigens. During immune responses, B cells differentiate into antibody-secreting cells, while naïve T cells differentiate into functionally specific effector cells [T helper 1 (Th1), Th2, Th17, and regulatory T cells]. However, enhanced or prolonged immune responses can result in autoimmune disorders, which are characterized by lymphocyte-mediated immune responses against self-antigens. Signal transduction of cytokines, which regulate the inflammatory cascades, is dependent on the members of the Janus family of protein kinases. Tyrosine kinase 2 (Tyk2) is associated with receptor subunits of immune-related cytokines, such as type I interferon, interleukin (IL)-6, IL-10, IL-12, and IL-23. Clinical studies on the therapeutic effects and the underlying mechanisms of Tyk2 inhibitors in autoimmune or chronic inflammatory diseases are currently ongoing. This review summarizes the findings of studies examining the role of Tyk2 in immune and/or inflammatory responses using *Tyk2*-deficient cells and mice.

Key Words: Tyrosine kinase 2; Cytokines; Signal transduction; Immune system; Inflammation

Grade E (Poor): 0

Received: March 27, 2021
Peer-review started: March 27, 2021
First decision: July 27, 2021
Revised: August 6, 2021
Accepted: December 22, 2021
Article in press: December 22, 2021
Published online: January 27, 2022

P-Reviewer: Todorovic-Rakovic N
S-Editor: Liu M
L-Editor: A
P-Editor: Liu M

Core Tip: Studies on murine *tyrosine kinase 2 (Tyk2)*-deficient models were reviewed to examine the role of Tyk2 dysregulation in human diseases. *Tyk2*-deficient mice exhibit reduced responses in several interleukin-12 (IL-12)/Th1- and IL-23/Th17-mediated models of diseases, including rheumatoid arthritis, multiple sclerosis, inflammatory bowel diseases, psoriasis, sarcoidosis, and delayed-type hypersensitivity. These findings demonstrate a broad contribution of Tyk2 to immune responses. Tyk2 represents a candidate for drug development by targeting both the IL-12/Th1 and IL-23/Th17 axes.

Citation: Muromoto R, Oritani K, Matsuda T. Current understanding of the role of tyrosine kinase 2 signaling in immune responses. *World J Biol Chem* 2022; 13(1): 1-14
URL: https://www.wjgnet.com/1949-8454/full/v13/i1/1.htm
DOI: https://dx.doi.org/10.4331/wjbc.v13.i1.1

INTRODUCTION

Cytokines function as effectors and regulate the proliferation, differentiation, and functions of immune cells and consequently aid in the clearance of invading pathogens. However, cytokines are also involved in the onset and development of autoimmune diseases[1]. Cytokine-specific cell surface receptors exhibit conformational changes upon activation, which result in activation of the Janus family of protein tyrosine kinases (Jaks). Activated Jaks promote the recruitment and phosphorylation of the transcription factor signal transducer and activator of transcription (STAT). Nuclear translocation of activated STATs induces the expression of cytokine-responsive genes. Thus, the Jak-STAT pathway transduces signals from various cytokine receptor superfamily members[2-4].

The Jak family comprises Jak1, Jak2, Jak3, and tyrosine kinase 2 (Tyk2), which are activated by distinct cytokines[2-4]. Jak1 binds to interferon (IFN), interleukin (IL)-6, and IL-10 receptors that contain a common γ chain and gp130 subunit, while Jak2 binds to IL-3 and erythropoietin, growth hormone, and prolactin hormone-like receptors. Tyk2 binds to IFN, IL-12, and IL-23 receptors. Jak3, whose expression is localized to hematopoietic cells, binds exclusively to receptors that contain common γ chains along with Jak1. Moreover, *Jak1* deficiency in mice results in perinatal lethality and impaired lymphocyte development[5]. The embryonic lethality in *Jak2*-deficient mice is attributed to insufficient definitive erythropoiesis[6]. *Jak3* deficiency results in dysfunctional mature T and B lymphocytes and leads to severe combined immunodeficiency[7,8]. Although *Tyk2*-deficient mice are viable, they are susceptible to viral infections[9,10].

Previous studies using experimental models, such as *Tyk2*-deficient mice have demonstrated that Tyk2 primarily functions in the IL-12 and IFN-α/β signaling pathways[9,10]. In humans, a mutation in *TYK2*, which causes an autosomal recessive form of hyper IgE syndrome (AR-HIES), affects the IL-23, IL-10, and IL-6 signal transduction pathways (Figure 1)[11]. Tyk2 is involved in both innate and acquired immunity. Here, the current knowledge on the involvement of Tyk2 in immune responses has been reviewed, and the potential clinical applications of Tyk2 inhibitors have been discussed.

ROLE OF TYK2 IN INFLAMMATORY RESPONSES

IFN system

Tyk2 was originally identified as a protein kinase that can compensate for the loss of IFN response in mutant fibroblasts[12]. IFN-α specifically activates Tyk2 and Jak1, which leads to the phosphorylation of STAT1 and STAT2 and the dimerization of activated STATs. The nuclear translocation of dimerized STATs induces the expression of target genes[3,13].

Type I IFNs are constitutively expressed in various cells, including macrophages. Although the constitutive expression of type I IFNs is low, they can regulate physiological cellular functions in an autocrine or a paracrine manner[14,15]. Tyk2

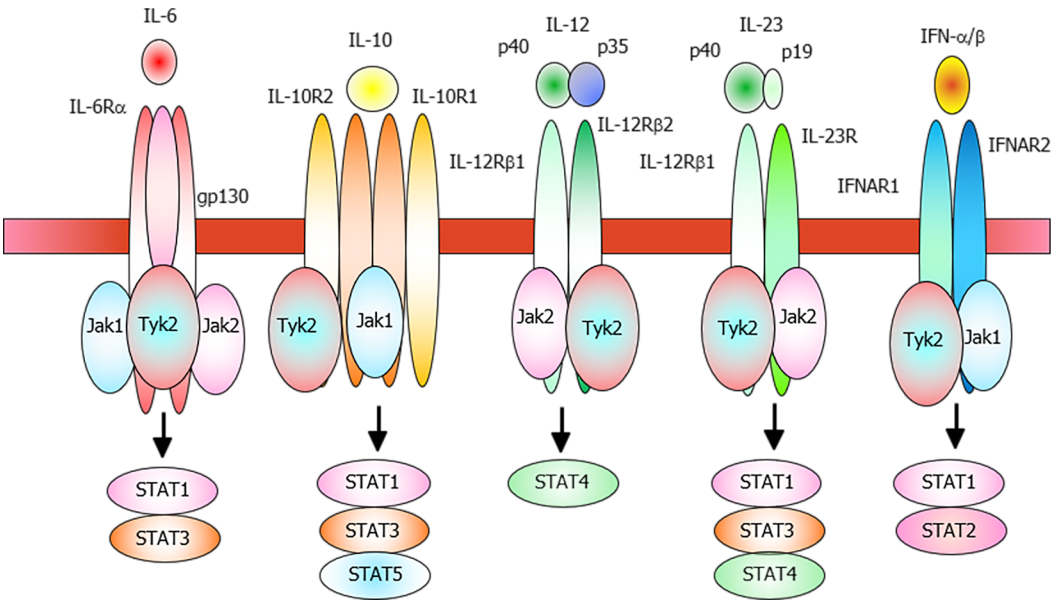

Figure 1 Schematic representation of the tyrosine kinase 2-related cytokine receptors. The IL-6 receptor, which comprises IL6RA (gp80) and IL6RB (gp130) subunits, activates signal transducer and activator of transcription (STAT)1 and STAT3 through interactions with Tyrosine kinase 2 (Tyk2), Janus family of protein tyrosine kinases 1 (Jak1), and Jak2. The IL-10 receptor, which comprises IL-10R1 and IL10-R2 subunits, activates STAT1, STAT3, and STAT5 through interactions with Tyk2 and Jak1. IL-12 is a heterodimeric cytokine comprising the IL-12p35 and IL-12p40 subunits. The IL-12 receptor, which comprises IL-12Rβ1 and IL-12Rβ2, mainly activates STAT4 through interactions with Tyk2 and Jak2. The IL-12p40 component of IL-23 can dimerize with IL-23p19 to form IL-23. The IL-23 receptor, which comprises IL-12Rβ1 and IL-23R subunits, activates STAT1, STAT3, and STAT4 through interactions with Tyk2 and Jak2. The type I IFN receptor, which comprises IFNAR1 and IFNAR2 subunits, activates STAT1 and STAT2 through interactions with Tyk2 and Jak1. STAT: Signal transducer and activator of transcription; Tyk2: Tyrosine kinase 2; Jak1: Janus family of protein tyrosine kinases 1.

promotes the constitutive production of type I IFNs in macrophages under steady-state conditions, as well as during the innate immune responses against bacterial components. The basal and lipopolysaccharide (LPS)-induced expression levels of type I IFN are dysregulated in *Tyk2*-deficient macrophages[16]. Moreover, *Tyk2*-deficient and *Ifnb*-deficient mice are resistant to high-dose LPS-induced lethal septic shock[16, 17]. Additionally, the expression of type I IFN-responsive genes, especially under steady-state conditions, was downregulated in *Tyk2*-deficient macrophages[18]. Therefore, Tyk2 is partially involved in macrophage activation by regulating autocrine and/or exogenous IFN production in the neighboring immune cells.

IL-12 and IL-23 systems

Helper T cells can be classified into the following two subsets based on their cytokine profiles: T helper 1 (Th1) and Th2 cells[19]. IL-12 and IL-4 promote the differentiation of naïve $CD4^+$ T cells into Th1 cells and Th2 cells, respectively. Heterodimeric IL-12 comprises covalently linked p35 and p40 subunits. Both IL-12 and IL-23 comprise the p40 subunit[20]. IL-23 (comprising p40 and unique p19 subunits) promotes the differentiation of Th17 cells, which secrete the effector cytokines IL-17, IL-21, and IL-22[21, 22]. Th17 cells can promote enhanced inflammatory responses to eliminate microbial pathogens. However, Th17 cells are considered highly pathogenic as excessive and prolonged activation of Th17 cells can result in autoimmune and inflammatory disorders, including inflammatory bowel diseases (IBD) and rheumatoid arthritis (RA), in humans (Figure 2)[21,22].

The activation of IL-12 receptor, which is associated with Tyk2 and Jak2, activates STAT4[23,24]. Phosphorylated Stat4 along with signals from the activated T cell receptor induces the expression of T-bet, which is a master transcriptional factor for Th1 differentiation[25]. IL-23, whose receptor is associated with Tyk2, induces the proliferation, survival, and functional maturation of Th17 cells[22,26] although Th17 cell differentiation is dependent on signals from TGF-β and IL-6 (Figure 3)[22]. STAT3, a major downstream effector of the Th17-related cytokine pathway, is critical for commitment to the Th17 Lineage, whereas STAT4 and STAT6 are essential for commitment to the Th1 and Th2 Lineages, respectively[27,28]. Additionally, *Tyk2*-deficient macrophages do not produce nitric oxide in response to LPS stimulation[16]. *Tyk2*-deficient dendritic cells do not produce IL-12 and IL-23 upon stimulation with CpG oligodeoxynucleotides and consequently cannot induce Th1 cell differentiation

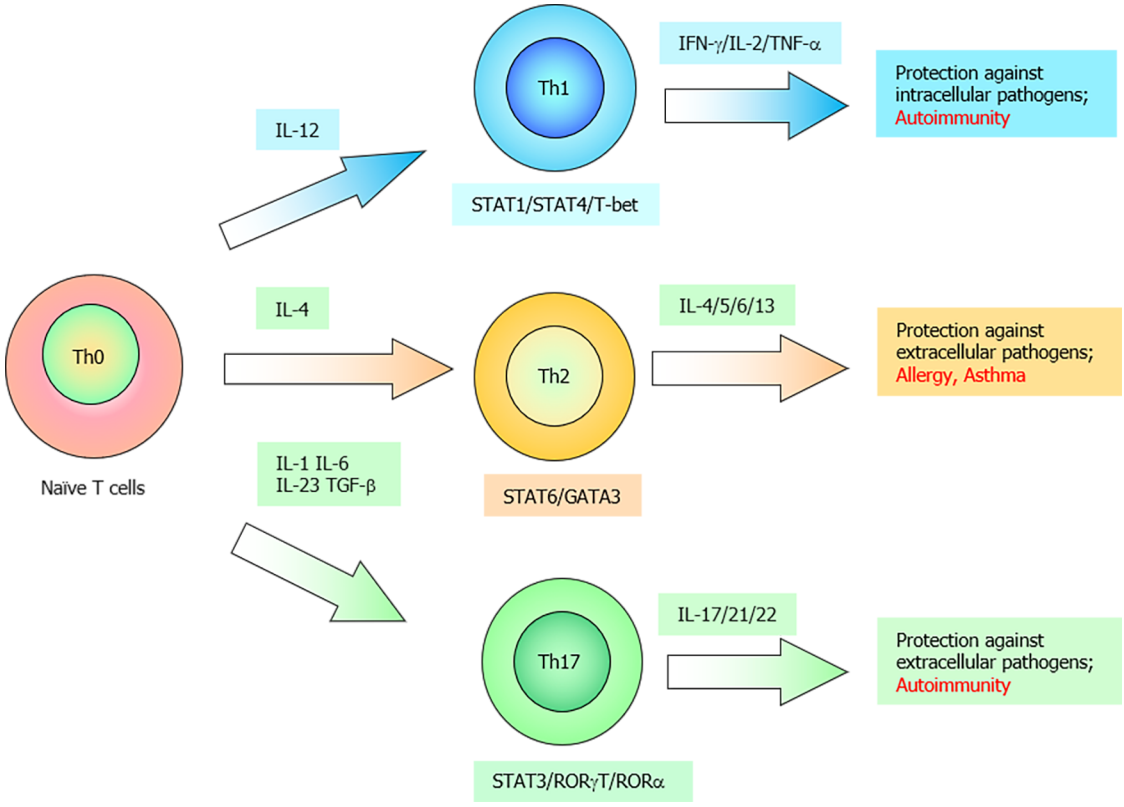

Figure 2 Schematic representation of naïve T cell differentiation into T helper 1, T helper 2, or T helper 17 cells depending on the cytokine profile. IL-12 promotes the differentiation of naïve T cells into Th1 cells. Th1 cells promote the clearance of intracellular pathogens and induce autoimmunity through the production of IFN-γ, IL-2, and TNF-α. Th1 differentiation is regulated by transcription factors such as signal transducer and activator of transcription (STAT)1, STAT4, and T-bet. IL-4 promotes the differentiation of naïve T cells into Th2 cells. Th2 cells promote the clearance of extracellular pathogens and induce allergic responses through the production of IL-4, IL-5, IL-6, and IL-13. Th2 differentiation is regulated by transcription factors such as STAT6 and GATA3. TGF-β, IL-6, and IL1 promote the differentiation of naïve T cells into Th17 cells, while IL-23 can maintain the Th17 phenotype. Th17 cells promote the clearance of extracellular pathogens and induce autoimmunity through the production of IL-17, IL-21, and IL-22. Th2 differentiation is regulated by transcription factors, such as STAT3, RORγt and RORα.

[29]. Therefore, Tyk2 is involved in the host defense response by regulating the production and function of both Th1 and Th17 cells.

Inhibitory effects of type I IFNs on B lymphopoiesis are mediated through the TYK2-DAXX axis

Interactions between IFN-α and its receptor promote potent antiviral and antiproliferative activities against the target cells[3,4]. IFN-α stimulation specifically activates Tyk2 and Jak1, which leads to the phosphorylation of STAT1 and STAT2. Nuclear translocation of phosphorylated STATs (in the form of homodimers or heterodimers) promotes target gene expression[3,4]. *Jak1*-deficient cells are not responsive to IFN-α stimulation[30], whereas *Tyk2*-deficient cells cannot inhibit lymphocyte growth[31]. Additionally, *Stat1*-deficient mice do not respond to IFN-α simulation[32,33], while *Stat2*-deficient mice are highly susceptible to viral infections[34].

Analysis of the colony forming unit (CFU) of bone marrow cells in the presence of IL-7 is a powerful tool to evaluate the growth capacity of B lymphocyte progenitors [35]. The CFU values of bone marrow cells in the presence of IL-7 were not markedly different between wild-type (WT) and *Tyk2*-deficient mice, which indicated that Tyk2 did not affect the number of IL-7-responsive B lymphocyte progenitors under steady-state conditions[31]. IFN-α, which is a potent inhibitor of IL-7-dependent growth of B lymphocyte progenitors, effectively inhibits B lymphocyte differentiation at the pro-B cell stage[36]. The CFU values of WT bone marrow cells in the presence of IL-7 markedly decreased upon stimulation with IFN-α. In contrast, the CFU values of *Tyk2*-deficient bone marrow cells in the presence of IL-7 did not decrease upon stimulation with IFN-α[31]. The knockout of *Tyk2* completely inhibited the IFN-α -induced elevation and nuclear accumulation of death-associated protein (Daxx)[31]. Daxx was originally identified as a Fas-binding protein[37] and it plays crucial roles in the type I IFN-induced growth suppression of B lymphocyte progenitors[38]. One study used the

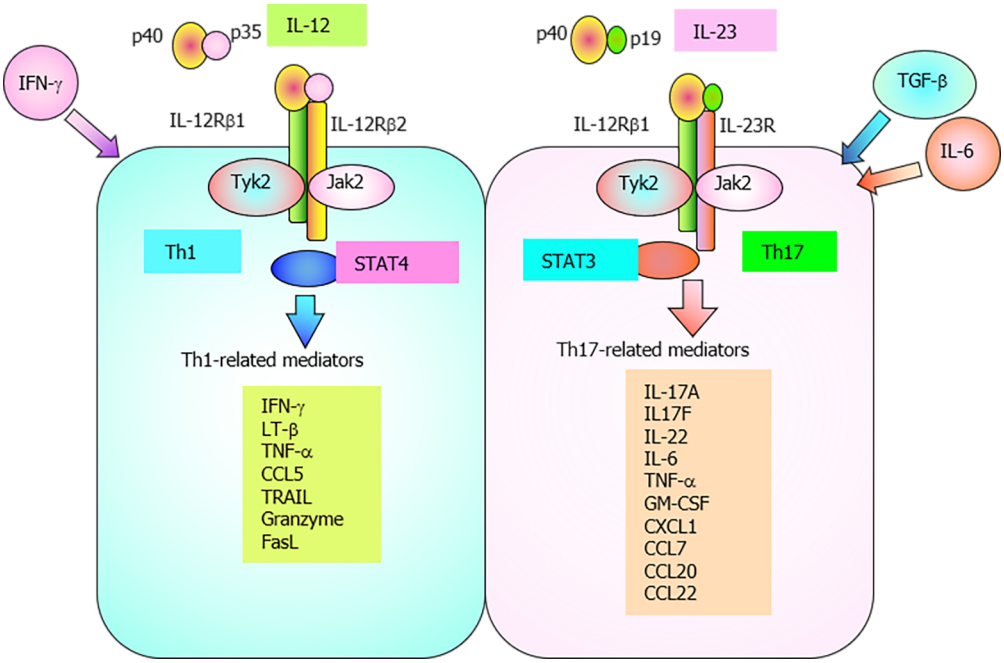

Figure 3 Illustration of interleukin-12 and interleukin-23, as well as their receptors and downstream signaling pathways. IL-12 and IL-23 share the p40 subunit, while their receptors share the IL-12Rβ1 subunit. The binding of IL-12 to its receptor induces the activation of Jak2 and Tyrosine kinase 2 (Tyk2), which results in signal transducer and activator of transcription (STAT)4 phosphorylation. Activated STAT4 promotes the differentiation of naïve Th cells into Th1 cells, which subsequently produce IFN-γ that is required for the development of Th1 immune response. The binding of IL-23 to its receptor induces the activation of Jak2 and Tyk2, which results in STAT3 phosphorylation. IL-23 induces the expression of IL-17A, IL-17F, and/or IL-22 and stabilizes Th17 cells. STAT: Signal transducer and activator of transcription.

sumoylation-defective Daxx KA mutant (Daxx K630/631A) to investigate the involvement of Daxx in decreasing the growth of Ba/F3 pro-B cells in the presence of IL-7 through IFN-α. The study demonstrated that Daxx KA is localized to the cytoplasm, whereas Daxx WT is localized to the nucleus[39]. Moreover, overexpression of Daxx KA conferred resistance to IFN-α -induced growth inhibition in a murine pro-B cell line Ba/F3. Treating Daxx KA-expressing Ba/F3 cells with leptomycin B, an exportin inhibitor, enhanced the nuclear localization of Daxx KA, and the growth of the cells was suppressed upon stimulation with IFN-α. Additionally, Daxx KA binds only weakly to promyelocytic leukemia protein (PML), which aids in the nuclear localization of Daxx. Conversely, overexpression of PML promotes the recruitment of Daxx to the PML nuclear bodies. A fusion protein comprising Daxx and a small ubiquitin-related modifier enhances the nuclear localization of Daxx and inhibits Ba/F3 cell growth. This indicates that IFN-α -induced inhibition of B lymphocyte progenitor growth requires nuclear localization of Daxx, which is dependent on sumoylation and interactions with PML. Therefore, the Tyk2-Daxx axis plays an essential role in IFN-α -induced growth inhibition of B lymphocyte progenitors.

PATHOLOGICAL SIGNIFICANCE OF TYK2 IN IMMUNE AND INFLAMMATORY DISEASES: DATA FROM MURINE EXPERIMENTAL MODELS

RA

RA is associated with joint inflammation and pain owing to a runaway immune system that elicits immune responses against the synovium of the joints of the hands, knees, or ankles. Murine experimental models for arthritis have provided useful information on various cellular and molecular mechanisms associated with RA[40].

Collagen-induced arthritis (CIA) mice are widely utilized as an experimental model for human RA[41]. Development of arthritis involves the production of autoantibodies in response to collagen and the subsequent inflammatory response against joints. Mice harboring *Tyk2* polymorphisms exhibit differential susceptibility to CIA[42,43]. B10.Q/Ai mice are highly susceptible to CIA, whereas B10.D1 mice are resistant. This suggests that *Tyk2* deficiency results in the defined clinical RA.

Monitoring of the inflammatory response in the anti-type II collagen (CII) antibody-induced arthritis (CAIA) experimental model provides useful information on the mechanisms of RA[44]. *Tyk2*-deficient mice are highly resistant to the development of CAIA. Histological analysis has revealed that *Tyk2* deficiency downregulated the inflammatory cell infiltration into the synovium[45]. Additionally, the production of IFN-γ, tumor necrosis factor (TNF)-α, IL-6, and matrix metalloproteinases (MMPs) was severely impaired in *Tyk2*-deficient mice[45]. TNF-α and IL-6, which are secreted by macrophages, function as pro-inflammatory cytokines in the CAIA model. MMPs, which are expressed in chondrocytes, synoviocytes, and macrophages, are reported to be involved in the degradation and damage of articular cartilage[46,47]. *Tyk2*-deficient macrophages cannot produce nitric oxide in response to LPS stimulation. Meanwhile, *Tyk2*-deficient dendritic cells cannot produce IL-12 and IL-23 in response to CpG oligodeoxynucleotides[29]. The potential mechanisms were analyzed using the anti-CII monoclonal antibody, which induced the phosphorylation of STAT3 and STAT4 in the draining lymph node cells. Phosphorylated STAT3 and STAT4 were detected in WT but not in *Tyk2*-deficient mice[45]. This suggests that Tyk2 promotes the production and downstream signaling of Th1/Th17-related cytokines, which are activated through STAT3 and STAT4.

Tyk2 deficiency markedly decreased the susceptibility to arthritis development in both CIA and CAIA murine models, which indicated that Tyk2 plays an important role in adaptive autoimmunity and inflammatory responses. Therefore, Tyk2 regulates multiple steps involved in the onset and development of RA.

Multiple sclerosis

Multiple sclerosis (MS) is characterized by the lack of myelin, a protective sheath covering nerve fibers, which leads to disruption of the communication between the brain and other tissues[48]. Patients with MS exhibit various symptoms, such as difficulty in walking and balancing, muscle weakness and spasticity, and loss of concentration and memory. The murine experimental autoimmune encephalomyelitis (EAE) model, which is an animal model for human MS, is triggered by immunization with myelin antigens or by the adoptive transfer of myelin-specific $CD4^+$ effector cells [49]. *Tyk2*-deficient mice exhibit decreased clinical scores and limited lymphocyte infiltration into the inflamed central nervous system[50]. The involvement of Tyk2 in EAE was confirmed using mice harboring different *Tyk2* polymorphisms. B10.D1 mice, which harbor the *Tyk2A* allele, are resistant to EAE development. The insufficient responses can be compensated by one copy of the *Tyk2G* allele from B10.Q/Ai mice [51].

IBD

Crohn's disease is characterized by inflammation of the digestive tract. Patients with Crohn's disease exhibit severe diarrhea, abdominal pain, fatigue, weight loss, and malnutrition[52]. Dextran sulfate sodium (DSS)-induced colitis, a mouse model for human Crohn's disease, is generated by supplementing mice with DSS through drinking water. The disease activity index and histological score were assessed using the combined scores of weight loss, consistency, and bleeding and acute clinical symptoms with diarrhea and/or extremely bloody stools[53]. Compared with that in WT DSS-induced colitis mice, disease development was delayed in *Tyk2*-deficient DSS-induced colitis mice[45]. Oral supplementation of DSS activates intestinal macrophages, which leads to enhanced production of inflammatory cytokines and chemokines. Subsequently, lymphocytes are recruited to the inflammatory sites and elicit Th1 and/or Th17 responses. During this inflammatory process, Tyk2 can regulate the functions of macrophages and dendritic cells, as well as the Th1 and Th17 responses. Indeed, the mRNA levels of DSS-induced Th1 cell-related or Th17 cell-related cytokines were significantly downregulated in the colon tissues of *Tyk2*-deficient mice [45]. A genome-wide association study identified *Tyk2* as a Crohn's disease susceptibility locus[54].

Ulcerative colitis is characterized by inflammation and ulcers in the large intestine and rectum. Patients with ulcerative colitis exhibit diarrhea with bloody stool, abdominal pain, fever, and body weight loss[55]. To model human ulcerative colitis in mice, 2,4,6-trinitrobenzene sulfonic acid (TNBS) is used[45]. WT mice treated with TNBS die within 3 days due to the induction of massive colitis. However, approximately 50% of *Tyk2*-deficient mice survive after treatment with TNBS. Additionally, the bodyweight of the surviving mice returned to the physiological range after recovery from diarrhea[45].

Therefore, Tyk2 is a key molecule for the development of IBD.

Psoriasis

Psoriasis is characterized by scaly erythematous lesions in the skin, epidermal hyperplasia, parakeratosis, and accumulation of inflammatory cells[56]. The inflammatory response is mediated by several cytokines, such as TNF-α, IL-17, and IL-23. The mouse model for human psoriasis was developed by treatment with imiquimod (IMQ), a ligand for TLR7[57]. *Il23p19*-deficient and *Il17a*–deficient mice exhibit decreased scores for erythema, scaling, and thickness upon treatment with IMQ, which suggests that the IL-23/Th17 axis and the Th17 cell-produced cytokines are essential for the development of skin abnormalities[57]. A genome-wide association study identified *Tyk2* as a psoriasis susceptibility locus[54]. *Tyk2* deficiency mitigates IMQ-induced enhanced ear thickness, which results from epidermal hyperplasia and inflammatory cell infiltration[45]. *Tyk2*-deficient mice exhibit markedly decreased numbers of $CD4^+IL\text{-}17^+$ or $CD4^+IFN\text{-}\gamma^+$ T cells in the draining lymph nodes and downregulated mRNA levels of Th17 cell-related cytokines upon treatment with IMQ [45].

The IL-23-induced skin inflammation mouse model is another promising model for human psoriasis[58]. In this IL-23-induced model, *Tyk2*-deficient mice exhibited reduced ear skin swelling, epidermal hyperplasia, Th17 and IL-22-producing Th22 cell infiltration compared with wild-type mice[45]. *Tyk2* deficiency downregulates the production of pro-inflammatory cytokines and psoriasis-related anti-microbial peptides.

IL-23 and IL-22 coordinate to promote skin inflammation[58,59]. Tyk2-mediated signals are essential for the induction of enhanced leukocyte infiltration and inflammatory cytokine production. Enhanced keratinocyte proliferation and differentiation are highly dependent on IL-17 and IL-22. Previous studies have reported that Tyk2 directly regulates IL-22-dependent processes as evidenced by the downregulation of STAT3 phosphorylation in *Tyk2* knockdown human keratinocyte HaCaT cells after IL-22 stimulation[45]. Therefore, Tyk2 has a critical role in the IL-22 signaling cascade that is involved in inducing epidermal hyperplasia.

IκB-ζ, an IL-17-induced protein encoded by *NFKBIZ*[60], is upregulated in the epidermal keratinocytes of psoriatic lesions[61]. *NFKBIZ* is located in the psoriasis susceptibility locus at 3q12.3[62]. IκB-ζ, a nuclear IκB family protein, positively or negatively modulates NF-κB-dependent and/or STAT3-dependent transcription[63-65]. Tyk2 is involved in IL-17–induced IκB-ζ expression in keratinocytes[66]. *Tyk2*-deficient mice exhibited only slight inflammation and downregulated mRNA levels of *Nfkbiz* upon treatment with IMQ. The catalytic activities of Tyk2 and STAT3 are required for IκB-ζ promoter activity in the HaCaT cells. The signaling pathways activated by IL-17 regulate mRNA stability[66-70]. ZC3H12A, which exhibits endoribonuclease activity, functions as a negative feedback regulator for inflammatory signaling[71-74]. The ubiquitin-proteasome pathway rapidly degrades ZC3H12A in IL-17-treated, IL-1β-treated, or IL-36–treated keratinocytes[72,74], which suggests that the stimulus-induced ZC3H12A downregulation can markedly suppress the inhibitory effects on mRNA expression.

Therefore, Tyk2 promotes the development of psoriasis by transducing IL-22 and IL-23 signals and regulating NFKBIZ along with the IL-17/ZC3H12A axis.

Sarcoidosis

Sarcoidosis is characterized by the aberrant accumulation of inflammatory cells, which typically form granulomas. Sarcoidosis usually begins in the lungs, skin, lymph nodes, eyes, heart, or other organs[75]. The murine model for human sarcoidosis is developed by intraperitoneally administering mice with heat-killed *Propionibacterium acnes* (*P. acnes*), which induces dense granulomas in the liver[76]. IL-12-IFN-γ axis is required for the induction since neither *Ifngr*-deficient nor *Il12p40*-deficient mice form hepatic granulomas after *P. acnes* injection[76]. *Tyk2*-deficient mice injected with *P. acnes* exhibit reduced serum IFN-γ level and decreased formation of hepatic granulomas compared with wild-type mice[45], indicating that Tyk2 has a role in *P. acnes*-induced granuloma formation.

Delayed-type hypersensitivity

Delayed-type hypersensitivity (DTH), which protects against various pathogens, such as mycobacteria, fungi, and parasites, contributes to transplant rejection and tumor immunity[77]. DTH is mainly dependent on T cells and develops 24–72 h after exposure to a foreign antigen. The DTH response analysis is based on a Th1/Th17 type model as the hypersensitivity response is defective in *Il12p40*-deficient and *Il23p19*-

deficient mice[78]. The sensitization phase is triggered by immunizing mice with a specific protein antigen (methylated BSA). The elicitation phase, which is initiated by the second injection of methylated BSA into the rear footpad of the pre-immunized mice, results in footpad swelling. Footpad swelling was significantly alleviated in *Tyk2* -deficient mice, which indicated the role of Tyk2 in DTH responses[45].

HIES

Tyk2 AR-HIES is a hereditary (autosomal recessive) disease involving a *Tyk2* mutation [79]. Patients with Tyk2 AR-HIES are characterized by repeated viral and mycobacterial infections, atopic dermatitis, and enhanced levels of IgE[11]. Therefore, Tyk2 may have a broader and more important role in immunological responses than expected from studies conducted using *Tyk2*-deficient mice.

POTENTIAL CLINICAL APPLICATIONS OF TYK2 INHIBITORS

The first *in vivo* evidence for the roles of Jaks in cytokine signaling originated from a human case study of severe combined immunodeficiency. Mutations in Jak3 or its receptor (a common g cytokine receptor chain) were detected in this case[80,81]. Another example is a somatic Jak2 valine-to-phenylalanine mutation (V617F), which is detected in more than 90% of the patients with polycythemia and some patients with essential thrombocythemia and primary myelofibrosis[82]. Activating point mutations in *Jak1* are detected in DNA samples from patients with acute lymphoblastic leukemia and are rarely observed in patients with acute myeloid leukemia[83]. Thus, dysregulation of the Jak-mediated signaling pathway is associated with the pathogenesis of different diseases, including hematological malignancies, autoimmune diseases, and immune-disrupted conditions. Studies on *Tyk2*-deficient mice or human patients with mutated *Tyk2* alleles have revealed that Tyk2 is a key player in the pathogenesis of autoimmune and/or inflammatory diseases.

Imatinib, a Bcr-Abl kinase inhibitor, exerts potent therapeutic effects in patients with chronic myelocytic leukemia[84]. Hence, various kinase inhibitors with strict selectivity and potency have been developed[85]. Jak inhibitors exert potent therapeutic effects by mitigating high levels of circulating immune/inflammatory cytokines. These results strongly suggest that Tyk2 is a potential therapeutic target for patients with immune and/or inflammatory diseases.

First-generation Jak inhibitors typically target two or three Jak types. Therefore, first-generation Jak inhibitors are associated with broader effects and more adverse events than the new-generation drugs, which specifically target one Jak type. Currently, several Jak inhibitors are used to treat various human diseases[86]. For example, ruxolitinib, an inhibitor of Jak1 and Jak2, has been approved to treat patients with myelofibrosis and polycythemia vera[87]. Tofacitinib, an inhibitor of Jak1, Jak2, and Jak3, has been approved to treat patients with RA, psoriatic arthritis, and ulcerative colitis[88]. Baricitinib, an inhibitor of Jak1 and Jak2, is used to treat patients with RA[89]. In methotrexate-inadequate responders, both tofacitinib and baricitinib provided enhanced therapeutic responses in patients with RA when compared with placebo[90]. In a phase 2 trial involving patients with psoriasis, the response rate to deucravacitinib (BMS-986165), a Tyk2 selective inhibitor[91], was significantly higher than that to placebo after 12 wk of administration. Treatment with BMS-986165 did not affect the blood cell counts or the serum levels of liver enzymes, lipids, and creatinine. However, BMS-986165 was associated with some severe adverse effects, such as malignant melanoma. Theoretically, therapeutic strategies targeting the immune system may increase the risk of infections from various pathogens, such as herpes zoster virus, cytomegalovirus, and Epstein–Barr virus. Therefore, further studies are needed to determine the long-term efficacy and safety of Tyk2 inhibitors. Additionally, clinical trials on Tyk2 inhibitors will aid in devising better therapeutic strategies for immune/inflammatory diseases than the currently marketed therapeutics.

CONCLUSION

This review summarized the involvement of Tyk2 in the immune system and its possible potential roles in the onset and development of immune and inflammatory diseases (Figure 4).

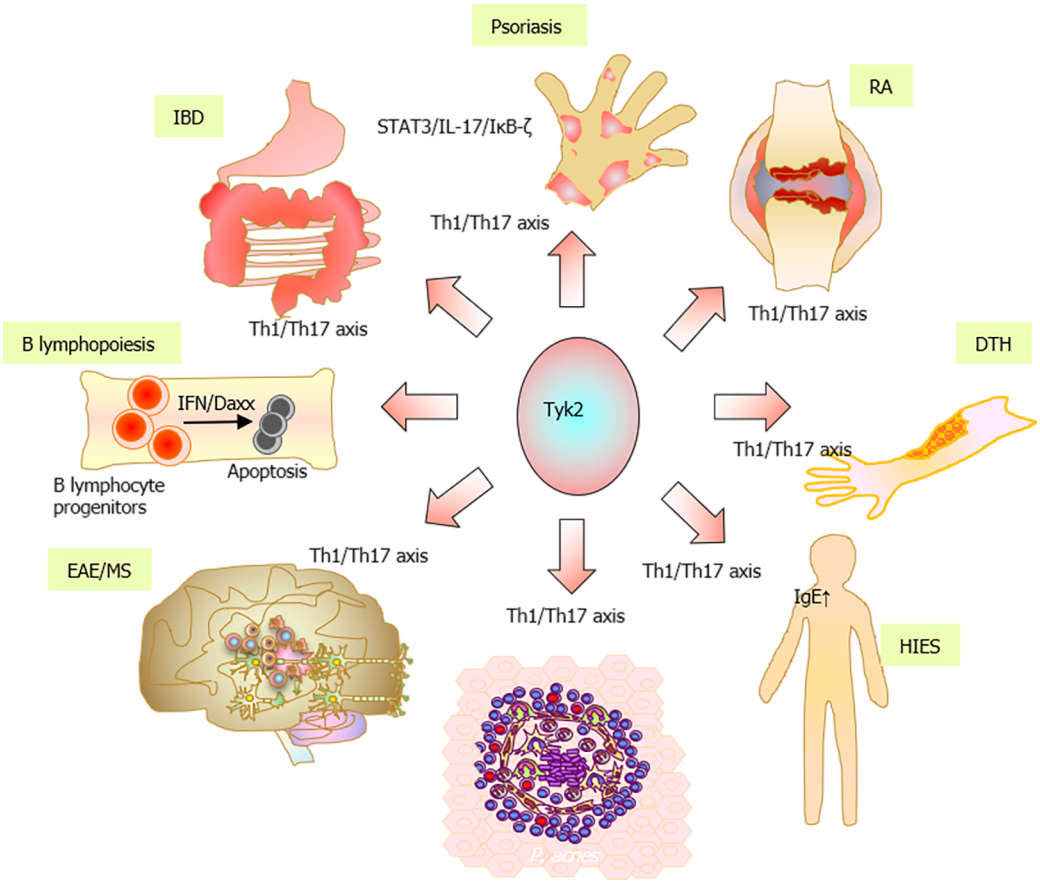

Figure 4 Schematic representation of the involvement of tyrosine kinase 2 in immune and inflammatory responses and its pathological significance. IBD: Inflammatory bowel diseases; RA: Rheumatoid arthritis; DTH: Delayed-type hypersensitivity; HIES: Hyper IgE syndrome; EAE: Experimental autoimmune encephalomyelitis; MS: Multiple sclerosis.

Studies on the *Tyk2*-deficient cells have revealed the involvement of the IFN system and IL-12/IL-23 axis. Constitutive production of a small amount of type I IFNs elicits a pro-inflammatory response against the invading pathogens and mitigates aberrant inflammation by promoting the expression of IL-10, a potent anti-inflammatory cytokine. Tyk2 is critical for maintaining the basal levels of IFNs. The IFN-α-induced decreased CFUs of bone marrow cells in the presence of IL-7 were also dependent on Tyk2. Tyk2 contributes to IFN-α signaling by promoting the nuclear translocation of Daxx and the formation of the Daxx/PML complex, which leads to growth inhibition. Additionally, Tyk2 interacts with the receptors for type I IFN, IL-6, IL-10, IL-12, and IL-23 (Figure 1). Moreover, Tyk2 is essential for IL-12-induced differentiation into Th1 cells, as well as IL-23-induced proliferation, survival, and functional maturation of Th17 cells. Additionally, Tyk2 mediates the production of nitric oxide in macrophages and IL-12 and IL-23 in dendritic cells after the invasion of pathogens.

Studies using *Tyk2*-deficient mice have revealed the potential involvement of Tyk2 in the onset and development of various immune and/or inflammatory disorders, such as RA, MS, IBD, psoriasis, sarcoidosis, and DTH. The development of most phenotypes in these models was mediated by Th1 and Th17 cells, whose differentiation and functions are highly dependent on Tyk2. Additionally, Tyk2 contributes to IL-17-induced IκB-ζ expression in IMQ-induced skin inflammation.

The experimental data summarized in this review along with the known clinical success of the novel Jak inhibitors indicate the therapeutic potential of Tyk2 inhibitors in the clinical setting. Further clinical trials are needed to examine the safety and efficacy profiles of Tyk2 inhibitors for treating psoriasis. Additionally, Tyk2 inhibitors are likely to be widely approved for various Th1/Th17-related immune/inflammatory diseases.

REFERENCES

1 **O'Shea JJ**, Ma A, Lipsky P. Cytokines and autoimmunity. *Nat Rev Immunol* 2002; **2**: 37-45 [PMID: 11905836 DOI: 10.1038/nri702]

2 **Ihle JN**. Cytokine receptor signalling. *Nature* 1995; **377**: 591-594 [PMID: 7566171 DOI: 10.1038/377591a0]

3 **Darnell JE**. STATs and gene regulation. *Science* 1997; **277**: 1630-1635 [PMID: 9287210 DOI: 10.1126/science.277.5332.1630]

4 **Stark GR**, Darnell JE Jr. The JAK-STAT pathway at twenty. *Immunity* 2012; **36**: 503-514 [PMID: 22520844 DOI: 10.1016/j.immuni.2012.03.013]

5 **Rodig SJ**, Meraz MA, White JM, Lampe PA, Riley JK, Arthur CD, King KL, Sheehan KC, Yin L, Pennica D, Johnson EM Jr, Schreiber RD. Disruption of the Jak1 gene demonstrates obligatory and nonredundant roles of the Jaks in cytokine-induced biologic responses. *Cell* 1998; **93**: 373-383 [PMID: 9590172 DOI: 10.1016/s0092-8674(00)81166-6]

6 **Parganas E**, Wang D, Stravopodis D, Topham DJ, Marine JC, Teglund S, Vanin EF, Bodner S, Colamonici OR, van Deursen JM, Grosveld G, Ihle JN. Jak2 is essential for signaling through a variety of cytokine receptors. *Cell* 1998; **93**: 385-395 [PMID: 9590173 DOI: 10.1016/s0092-8674(00)81167-8]

7 **Nosaka T**, van Deursen JM, Tripp RA, Thierfelder WE, Witthuhn BA, McMickle AP, Doherty PC, Grosveld GC, Ihle JN. Defective lymphoid development in mice lacking Jak3. *Science* 1995; **270**: 800-802 [PMID: 7481769 DOI: 10.1126/science.270.5237.800]

8 **Macchi P**, Villa A, Giliani S, Sacco MG, Frattini A, Porta F, Ugazio AG, Johnston JA, Candotti F, O'Shea JJ. Mutations of Jak-3 gene in patients with autosomal severe combined immune deficiency (SCID). *Nature* 1995; **377**: 65-68 [PMID: 7659163 DOI: 10.1038/377065a0]

9 **Shimoda K**, Kato K, Aoki K, Matsuda T, Miyamoto A, Shibamori M, Yamashita M, Numata A, Takase K, Kobayashi S, Shibata S, Asano Y, Gondo H, Sekiguchi K, Nakayama K, Nakayama T, Okamura T, Okamura S, Niho Y. Tyk2 plays a restricted role in IFN alpha signaling, although it is required for IL-12-mediated T cell function. *Immunity* 2000; **13**: 561-571 [PMID: 11070174 DOI: 10.1016/s1074-7613(00)00055-8]

10 **Karaghiosoff M**, Neubauer H, Lassnig C, Kovarik P, Schindler H, Pircher H, McCoy B, Bogdan C, Decker T, Brem G, Pfeffer K, Müller M. Partial impairment of cytokine responses in Tyk2-deficient mice. *Immunity* 2000; **13**: 549-560 [PMID: 11070173 DOI: 10.1016/s1074-7613(00)00054-6]

11 **Minegishi Y**, Saito M, Morio T, Watanabe K, Agematsu K, Tsuchiya S, Takada H, Hara T, Kawamura N, Ariga T, Kaneko H, Kondo N, Tsuge I, Yachie A, Sakiyama Y, Iwata T, Bessho F, Ohishi T, Joh K, Imai K, Kogawa K, Shinohara M, Fujieda M, Wakiguchi H, Pasic S, Abinun M, Ochs HD, Renner ED, Jansson A, Belohradsky BH, Metin A, Shimizu N, Mizutani S, Miyawaki T, Nonoyama S, Karasuyama H. Human tyrosine kinase 2 deficiency reveals its requisite roles in multiple cytokine signals involved in innate and acquired immunity. *Immunity* 2006; **25**: 745-755 [PMID: 17088085 DOI: 10.1016/j.immuni.2006.09.009]

12 **Velazquez L**, Fellous M, Stark GR, Pellegrini S. A protein tyrosine kinase in the interferon alpha/beta signaling pathway. *Cell* 1992; **70**: 313-322 [PMID: 1386289 DOI: 10.1016/0092-8674(92)90105-l]

13 **Darnell JE Jr**, Kerr IM, Stark GR. Jak-STAT pathways and transcriptional activation in response to IFNs and other extracellular signaling proteins. *Science* 1994; **264**: 1415-1421 [PMID: 8197455 DOI: 10.1126/science.8197455]

14 **Gough DJ**, Messina NL, Clarke CJ, Johnstone RW, Levy DE. Constitutive type I interferon modulates homeostatic balance through tonic signaling. *Immunity* 2012; **36**: 166-174 [PMID: 22365663 DOI: 10.1016/j.immuni.2012.01.011]

15 **Taniguchi T**, Takaoka A. A weak signal for strong responses: interferon-alpha/beta revisited. *Nat Rev Mol Cell Biol* 2001; **2**: 378-386 [PMID: 11331912 DOI: 10.1038/35073080]

16 **Karaghiosoff M**, Steinborn R, Kovarik P, Kriegshäuser G, Baccarini M, Donabauer B, Reichart U, Kolbe T, Bogdan C, Leanderson T, Levy D, Decker T, Müller M. Central role for type I interferons and Tyk2 in lipopolysaccharide-induced endotoxin shock. *Nat Immunol* 2003; **4**: 471-477 [PMID: 12679810 DOI: 10.1038/ni910]

17 **Kamezaki K**, Shimoda K, Numata A, Matsuda T, Nakayama K, Harada M. The role of Tyk2, Stat1 and Stat4 in LPS-induced endotoxin signals. *Int Immunol* 2004; **16**: 1173-1179 [PMID: 15226272 DOI: 10.1093/intimm/dxh118]

18 **Vogl C**, Flatt T, Fuhrmann B, Hofmann E, Wallner B, Stiefvater R, Kovarik P, Strobl B, Müller M. Transcriptome analysis reveals a major impact of JAK protein tyrosine kinase 2 (Tyk2) on the expression of interferon-responsive and metabolic genes. *BMC Genomics* 2010; **11**: 199 [PMID: 20338026 DOI: 10.1186/1471-2164-11-199]

19 **Mosmann TR**, Coffman RL. TH1 and TH2 cells: different patterns of lymphokine secretion lead to different functional properties. *Annu Rev Immunol* 1989; **7**: 145-173 [PMID: 2523712 DOI: 10.1146/annurev.iy.07.040189.001045]

20 **Oppmann B**, Lesley R, Blom B, Timans JC, Xu Y, Hunte B, Vega F, Yu N, Wang J, Singh K, Zonin F, Vaisberg E, Churakova T, Liu M, Gorman D, Wagner J, Zurawski S, Liu Y, Abrams JS, Moore KW, Rennick D, de Waal-Malefyt R, Hannum C, Bazan JF, Kastelein RA. Novel p19 protein engages IL-12p40 to form a cytokine, IL-23, with biological activities similar as well as distinct from IL-12. *Immunity* 2000; **13**: 715-725 [PMID: 11114383 DOI: 10.1016/s1074-7613(00)00070-4]

21 **Bettelli E**, Korn T, Oukka M, Kuchroo VK. Induction and effector functions of T(H)17 cells. *Nature*

2008; **453**: 1051-1057 [PMID: 18563156 DOI: 10.1038/nature07036]
22 **Korn T**, Bettelli E, Oukka M, Kuchroo VK. IL-17 and Th17 Cells. *Annu Rev Immunol* 2009; **27**: 485-517 [PMID: 19132915 DOI: 10.1146/annurev.immunol.021908.132710]
23 **Bacon CM**, Petricoin EF 3rd, Ortaldo JR, Rees RC, Larner AC, Johnston JA, O'Shea JJ. Interleukin 12 induces tyrosine phosphorylation and activation of STAT4 in human lymphocytes. *Proc Natl Acad Sci U S A* 1995; **92**: 7307-7311 [PMID: 7638186 DOI: 10.1073/pnas.92.16.7307]
24 **Bacon CM**, McVicar DW, Ortaldo JR, Rees RC, O'Shea JJ, Johnston JA. Interleukin 12 (IL-12) induces tyrosine phosphorylation of JAK2 and TYK2: differential use of Janus family tyrosine kinases by IL-2 and IL-12. *J Exp Med* 1995; **181**: 399-404 [PMID: 7528775 DOI: 10.1084/jem.181.1.399]
25 **Robinson DS**, O'Garra A. Further checkpoints in Th1 development. *Immunity* 2002; **16**: 755-758 [PMID: 12121657 DOI: 10.1016/s1074-7613(02)00331-x]
26 **Parham C**, Chirica M, Timans J, Vaisberg E, Travis M, Cheung J, Pflanz S, Zhang R, Singh KP, Vega F, To W, Wagner J, O'Farrell AM, McClanahan T, Zurawski S, Hannum C, Gorman D, Rennick DM, Kastelein RA, de Waal Malefyt R, Moore KW. A receptor for the heterodimeric cytokine IL-23 is composed of IL-12Rbeta1 and a novel cytokine receptor subunit, IL-23R. *J Immunol* 2002; **168**: 5699-5708 [PMID: 12023369 DOI: 10.4049/jimmunol.168.11.5699]
27 **Harris TJ**, Grosso JF, Yen HR, Xin H, Kortylewski M, Albesiano E, Hipkiss EL, Getnet D, Goldberg MV, Maris CH, Housseau F, Yu H, Pardoll DM, Drake CG. Cutting edge: An in vivo requirement for STAT3 signaling in TH17 development and TH17-dependent autoimmunity. *J Immunol* 2007; **179**: 4313-4317 [PMID: 17878325 DOI: 10.4049/jimmunol.179.7.4313]
28 **Wilson CB**, Rowell E, Sekimata M. Epigenetic control of T-helper-cell differentiation. *Nat Rev Immunol* 2009; **9**: 91-105 [PMID: 19151746 DOI: 10.1038/nri2487]
29 **Tokumasa N**, Suto A, Kagami S, Furuta S, Hirose K, Watanabe N, Saito Y, Shimoda K, Iwamoto I, Nakajima H. Expression of Tyk2 in dendritic cells is required for IL-12, IL-23, and IFN-gamma production and the induction of Th1 cell differentiation. *Blood* 2007; **110**: 553-560 [PMID: 17395783 DOI: 10.1182/blood-2006-11-059246]
30 **Müller M**, Briscoe J, Laxton C, Guschin D, Ziemiecki A, Silvennoinen O, Harpur AG, Barbieri G, Witthuhn BA, Schindler C. The protein tyrosine kinase JAK1 complements defects in interferon-alpha/beta and -gamma signal transduction. *Nature* 1993; **366**: 129-135 [PMID: 8232552 DOI: 10.1038/366129a0]
31 **Shimoda K**, Kamesaki K, Numata A, Aoki K, Matsuda T, Oritani K, Tamiya S, Kato K, Takase K, Imamura R, Yamamoto T, Miyamoto T, Nagafuji K, Gondo H, Nagafuchi S, Nakayama K, Harada M. Cutting edge: tyk2 is required for the induction and nuclear translocation of Daxx which regulates IFN-alpha-induced suppression of B lymphocyte formation. *J Immunol* 2002; **169**: 4707-4711 [PMID: 12391177 DOI: 10.4049/jimmunol.169.9.4707]
32 **Meraz MA**, White JM, Sheehan KC, Bach EA, Rodig SJ, Dighe AS, Kaplan DH, Riley JK, Greenlund AC, Campbell D, Carver-Moore K, DuBois RN, Clark R, Aguet M, Schreiber RD. Targeted disruption of the Stat1 gene in mice reveals unexpected physiologic specificity in the JAK-STAT signaling pathway. *Cell* 1996; **84**: 431-442 [PMID: 8608597 DOI: 10.1016/s0092-8674(00)81288-x]
33 **Durbin JE**, Hackenmiller R, Simon MC, Levy DE. Targeted disruption of the mouse Stat1 gene results in compromised innate immunity to viral disease. *Cell* 1996; **84**: 443-450 [PMID: 8608598 DOI: 10.1016/s0092-8674(00)81289-1]
34 **Park C**, Li S, Cha E, Schindler C. Immune response in Stat2 knockout mice. *Immunity* 2000; **13**: 795-804 [PMID: 11163195 DOI: 10.1016/s1074-7613(00)00077-7]
35 **Namen AE**, Lupton S, Hjerrild K, Wignall J, Mochizuki DY, Schmierer A, Mosley B, March CJ, Urdal D, Gillis S. Stimulation of B-cell progenitors by cloned murine interleukin-7. *Nature* 1988; **333**: 571-573 [PMID: 3259677 DOI: 10.1038/333571a0]
36 **Lin Q**, Dong C, Cooper MD. Impairment of T and B cell development by treatment with a type I interferon. *J Exp Med* 1998; **187**: 79-87 [PMID: 9419213 DOI: 10.1084/jem.187.1.79]
37 **Yang X**, Khosravi-Far R, Chang HY, Baltimore D. Daxx, a novel Fas-binding protein that activates JNK and apoptosis. *Cell* 1997; **89**: 1067-1076 [PMID: 9215629 DOI: 10.1016/s0092-8674(00)80294-9]
38 **Gongora R**, Stephan RP, Zhang Z, Cooper MD. An essential role for Daxx in the inhibition of B lymphopoiesis by type I interferons. *Immunity* 2001; **14**: 727-737 [PMID: 11420043 DOI: 10.1016/s1074-7613(01)00152-2]
39 **Muromoto R**, Ishida M, Sugiyama K, Sekine Y, Oritani K, Shimoda K, Matsuda T. Sumoylation of Daxx regulates IFN-induced growth suppression of B lymphocytes and the hormone receptor-mediated transactivation. *J Immunol* 2006; **177**: 1160-1170 [PMID: 16818774 DOI: 10.4049/jimmunol.177.2.1160]
40 **Gay S**. Rheumatoid arthritis. *Curr Opin Rheumatol* 2001; **13**: 191-192 [PMID: 11333347 DOI: 10.1097/00002281-200105000-00007]
41 **Courtenay JS**, Dallman MJ, Dayan AD, Martin A, Mosedale B. Immunisation against heterologous type II collagen induces arthritis in mice. *Nature* 1980; **283**: 666-668 [PMID: 6153460 DOI: 10.1038/283666a0]
42 **Ortmann R**, Smeltz R, Yap G, Sher A, Shevach EM. A heritable defect in IL-12 signaling in B10.Q/J mice. I. In vitro analysis. *J Immunol* 2001; **166**: 5712-5719 [PMID: 11313413 DOI: 10.4049/jimmunol.166.9.5712]

43 **Yap GS**, Ortmann R, Shevach E, Sher A. A heritable defect in IL-12 signaling in B10.Q/J mice. II. Effect on acute resistance to Toxoplasma gondii and rescue by IL-18 treatment. *J Immunol* 2001; **166**: 5720-5725 [PMID: 11313414 DOI: 10.4049/jimmunol.166.9.5720]

44 **Khachigian LM**. Collagen antibody-induced arthritis. *Nat Protoc* 2006; **1**: 2512-2516 [PMID: 17406499 DOI: 10.1038/nprot.2006.393]

45 **Muromoto R**, Oritani K, Matsuda T. Tyk2-mediated homeostatic control by regulating the PGE2-PKA-IL-10 axis. *AIMS Allergy Immunol* 2021; **5**: 175-183 [DOI: 10.3934/Allergy.2021013]

46 **Itoh T**, Matsuda H, Tanioka M, Kuwabara K, Itohara S, Suzuki R. The role of matrix metalloproteinase-2 and matrix metalloproteinase-9 in antibody-induced arthritis. *J Immunol* 2002; **169**: 2643-2647 [PMID: 12193736 DOI: 10.4049/jimmunol.169.5.2643]

47 **Paniagua RT**, Chang A, Mariano MM, Stein EA, Wang Q, Lindstrom TM, Sharpe O, Roscow C, Ho PP, Lee DM, Robinson WH. c-Fms-mediated differentiation and priming of monocyte lineage cells play a central role in autoimmune arthritis. *Arthritis Res Ther* 2010; **12**: R32 [PMID: 20181277 DOI: 10.1186/ar2940]

48 **Owens B**. Multiple sclerosis. *Nature* 2016; **540**: S1 [PMID: 27902684 DOI: 10.1038/540S1a]

49 **Zamvil SS**, Steinman L. The T lymphocyte in experimental allergic encephalomyelitis. *Annu Rev Immunol* 1990; **8**: 579-621 [PMID: 2188675 DOI: 10.1146/annurev.iy.08.040190.003051]

50 **Oyamada A**, Ikebe H, Itsumi M, Saiwai H, Okada S, Shimoda K, Iwakura Y, Nakayama KI, Iwamoto Y, Yoshikai Y, Yamada H. Tyrosine kinase 2 plays critical roles in the pathogenic CD4 T cell responses for the development of experimental autoimmune encephalomyelitis. *J Immunol* 2009; **183**: 7539-7546 [PMID: 19917699 DOI: 10.4049/jimmunol.0902740]

51 **Spach KM**, Noubade R, McElvany B, Hickey WF, Blankenhorn EP, Teuscher C. A single nucleotide polymorphism in Tyk2 controls susceptibility to experimental allergic encephalomyelitis. *J Immunol* 2009; **182**: 7776-7783 [PMID: 19494301 DOI: 10.4049/jimmunol.0900142]

52 **Roda G**, Chien Ng S, Kotze PG, Argollo M, Panaccione R, Spinelli A, Kaser A, Peyrin-Biroulet L, Danese S. Crohn's disease. *Nat Rev Dis Primers* 2020; **6**: 22 [PMID: 32242028 DOI: 10.1038/s41572-020-0156-2]

53 **Wirtz S**, Neurath MF. Mouse models of inflammatory bowel disease. *Adv Drug Deliv Rev* 2007; **59**: 1073-1083 [PMID: 17825455 DOI: 10.1016/j.addr.2007.07.003]

54 **Ellinghaus D**, Ellinghaus E, Nair RP, Stuart PE, Esko T, Metspalu A, Debrus S, Raelson JV, Tejasvi T, Belouchi M, West SL, Barker JN, Kõks S, Kingo K, Balschun T, Palmieri O, Annese V, Gieger C, Wichmann HE, Kabesch M, Trembath RC, Mathew CG, Abecasis GR, Weidinger S, Nikolaus S, Schreiber S, Elder JT, Weichenthal M, Nothnagel M, Franke A. Combined analysis of genome-wide association studies for Crohn disease and psoriasis identifies seven shared susceptibility loci. *Am J Hum Genet* 2012; **90**: 636-647 [PMID: 22482804 DOI: 10.1016/j.ajhg.2012.02.020]

55 **Kobayashi T**, Siegmund B, Le Berre C, Wei SC, Ferrante M, Shen B, Bernstein CN, Danese S, Peyrin-Biroulet L, Hibi T. Ulcerative colitis. *Nat Rev Dis Primers* 2020; **6**: 74 [PMID: 32913180 DOI: 10.1038/s41572-020-0205-x]

56 **Lowes MA**, Bowcock AM, Krueger JG. Pathogenesis and therapy of psoriasis. *Nature* 2007; **445**: 866-873 [PMID: 17314973 DOI: 10.1038/nature05663]

57 **van der Fits L**, Mourits S, Voerman JS, Kant M, Boon L, Laman JD, Cornelissen F, Mus AM, Florencia E, Prens EP, Lubberts E. Imiquimod-induced psoriasis-like skin inflammation in mice is mediated *via* the IL-23/IL-17 axis. *J Immunol* 2009; **182**: 5836-5845 [PMID: 19380832 DOI: 10.4049/jimmunol.0802999]

58 **Zheng Y**, Danilenko DM, Valdez P, Kasman I, Eastham-Anderson J, Wu J, Ouyang W. Interleukin-22, a T(H)17 cytokine, mediates IL-23-induced dermal inflammation and acanthosis. *Nature* 2007; **445**: 648-651 [PMID: 17187052 DOI: 10.1038/nature05505]

59 **Rizzo HL**, Kagami S, Phillips KG, Kurtz SE, Jacques SL, Blauvelt A. IL-23-mediated psoriasis-like epidermal hyperplasia is dependent on IL-17A. *J Immunol* 2011; **186**: 1495-1502 [PMID: 21172868 DOI: 10.4049/jimmunol.1001001]

60 **Muromoto R**, Hirao T, Tawa K, Hirashima K, Kon S, Kitai Y, Matsuda T. IL-17A plays a central role in the expression of psoriasis signature genes through the induction of IκB-ζ in keratinocytes. *Int Immunol* 2016; **28**: 443-452 [PMID: 26944069 DOI: 10.1093/intimm/dxw011]

61 **Johansen C**, Mose M, Ommen P, Bertelsen T, Vinter H, Hailfinger S, Lorscheid S, Schulze-Osthoff K, Iversen L. IκBζ is a key driver in the development of psoriasis. *Proc Natl Acad Sci U S A* 2015; **112**: E5825-E5833 [PMID: 26460049 DOI: 10.1073/pnas.1509971112]

62 **Tsoi LC**, Spain SL, Ellinghaus E, Stuart PE, Capon F, Knight J, Tejasvi T, Kang HM, Allen MH, Lambert S, Stoll SW, Weidinger S, Gudjonsson JE, Koks S, Kingo K, Esko T, Das S, Metspalu A, Weichenthal M, Enerback C, Krueger GG, Voorhees JJ, Chandran V, Rosen CF, Rahman P, Gladman DD, Reis A, Nair RP, Franke A, Barker JNWN, Abecasis GR, Trembath RC, Elder JT. Enhanced meta-analysis and replication studies identify five new psoriasis susceptibility loci. *Nat Commun* 2015; **6**: 7001 [PMID: 25939698 DOI: 10.1038/ncomms8001]

63 **Müller A**, Hennig A, Lorscheid S, Grondona P, Schulze-Osthoff K, Hailfinger S, Kramer D. IκBζ is a key transcriptional regulator of IL-36-driven psoriasis-related gene expression in keratinocytes. *Proc Natl Acad Sci U S A* 2018; **115**: 10088-10093 [PMID: 30224457 DOI: 10.1073/pnas.1801377115]

64 **Yamazaki S**, Muta T, Matsuo S, Takeshige K. Stimulus-specific induction of a novel nuclear factor-kappaB regulator, IkappaB-zeta, *via* Toll/Interleukin-1 receptor is mediated by mRNA stabilization. *J Biol Chem* 2005; **280**: 1678-1687 [PMID: 15522867 DOI: 10.1074/jbc.M409983200]

65 **Okuma A**, Hoshino K, Ohba T, Fukushi S, Aiba S, Akira S, Ono M, Kaisho T, Muta T. Enhanced

apoptosis by disruption of the STAT3-IκB-ζ signaling pathway in epithelial cells induces Sjögren's syndrome-like autoimmune disease. *Immunity* 2013; **38**: 450-460 [PMID: 23453632 DOI: 10.1016/j.immuni.2012.11.016]

66 **Muromoto R**, Tawa K, Ohgakiuchi Y, Sato A, Saino Y, Hirashima K, Minoguchi H, Kitai Y, Kashiwakura JI, Shimoda K, Oritani K, Matsuda T. IκB-ζ Expression Requires Both TYK2/STAT3 Activity and IL-17-Regulated mRNA Stabilization. *Immunohorizons* 2019; **3**: 172-185 [PMID: 31356171 DOI: 10.4049/immunohorizons.1900023]

67 **Hartupee J**, Liu C, Novotny M, Li X, Hamilton T. IL-17 enhances chemokine gene expression through mRNA stabilization. *J Immunol* 2007; **179**: 4135-4141 [PMID: 17785852 DOI: 10.4049/jimmunol.179.6.4135]

68 **Herjan T**, Hong L, Bubenik J, Bulek K, Qian W, Liu C, Li X, Chen X, Yang H, Ouyang S, Zhou H, Zhao J, Vasu K, Cockman E, Aronica M, Asosingh K, Licatalosi DD, Qin J, Fox PL, Hamilton TA, Driscoll D. IL-17-receptor-associated adaptor Act1 directly stabilizes mRNAs to mediate IL-17 inflammatory signaling. *Nat Immunol* 2018; **19**: 354-365 [PMID: 29563620 DOI: 10.1038/s41590-018-0071-9]

69 **Amatya N**, Childs EE, Cruz JA, Aggor FEY, Garg AV, Berman AJ, Gudjonsson JE, Atasoy U, Gaffen SL. IL-17 integrates multiple self-reinforcing, feed-forward mechanisms through the RNA binding protein Arid5a. *Sci Signal* 2018; **11** [PMID: 30301788 DOI: 10.1126/scisignal.aat4617]

70 **Dhamija S**, Winzen R, Doerrie A, Behrens G, Kuehne N, Schauerte C, Neumann E, Dittrich-Breiholz O, Kracht M, Holtmann H. Interleukin-17 (IL-17) and IL-1 activate translation of overlapping sets of mRNAs, including that of the negative regulator of inflammation, MCPIP1. *J Biol Chem* 2013; **288**: 19250-19259 [PMID: 23658019 DOI: 10.1074/jbc.M113.452649]

71 **Matsushita K**, Takeuchi O, Standley DM, Kumagai Y, Kawagoe T, Miyake T, Satoh T, Kato H, Tsujimura T, Nakamura H, Akira S. Zc3h12a is an RNase essential for controlling immune responses by regulating mRNA decay. *Nature* 2009; **458**: 1185-1190 [PMID: 19322177 DOI: 10.1038/nature07924]

72 **Iwasaki H**, Takeuchi O, Teraguchi S, Matsushita K, Uehata T, Kuniyoshi K, Satoh T, Saitoh T, Matsushita M, Standley DM, Akira S. The IκB kinase complex regulates the stability of cytokine-encoding mRNA induced by TLR-IL-1R by controlling degradation of regnase-1. *Nat Immunol* 2011; **12**: 1167-1175 [PMID: 22037600 DOI: 10.1038/ni.2137]

73 **Monin L**, Gudjonsson JE, Childs EE, Amatya N, Xing X, Verma AH, Coleman BM, Garg AV, Killeen M, Mathers A, Ward NL, Gaffen SL. MCPIP1/Regnase-1 Restricts IL-17A- and IL-17C-Dependent Skin Inflammation. *J Immunol* 2017; **198**: 767-775 [PMID: 27920272 DOI: 10.4049/jimmunol.1601551]

74 **Takaishi M**, Satoh T, Akira S, Sano S. Regnase-1, an Immunomodulator, Limits the IL-36/IL-36R Autostimulatory Loop in Keratinocytes to Suppress Skin Inflammation. *J Invest Dermatol* 2018; **138**: 1439-1442 [PMID: 29339122 DOI: 10.1016/j.jid.2017.12.033]

75 **Grunewald J**, Grutters JC, Arkema EV, Saketkoo LA, Moller DR, Müller-Quernheim J. Sarcoidosis. *Nat Rev Dis Primers* 2019; **5**: 45 [PMID: 31273209 DOI: 10.1038/s41572-019-0096-x]

76 **Tsutsui H**, Imamura M, Fujimoto J, Nakanishi K. The TLR4/TRIF-Mediated Activation of NLRP3 Inflammasome Underlies Endotoxin-Induced Liver Injury in Mice. *Gastroenterol Res Pract* 2010; **2010**: 641865 [PMID: 20634907 DOI: 10.1155/2010/641865]

77 **Black CA**. Delayed type hypersensitivity: current theories with an historic perspective. *Dermatol Online J* 1999; **5**: 7 [PMID: 10673450]

78 **Ghilardi N**, Kljavin N, Chen Q, Lucas S, Gurney AL, De Sauvage FJ. Compromised humoral and delayed-type hypersensitivity responses in IL-23-deficient mice. *J Immunol* 2004; **172**: 2827-2833 [PMID: 14978083 DOI: 10.4049/jimmunol.172.5.2827]

79 **Minegishi Y**. Hyper-IgE syndrome. *Curr Opin Immunol* 2009; **21**: 487-492 [PMID: 19717292 DOI: 10.1016/j.coi.2009.07.013]

80 **Russell SM**, Tayebi N, Nakajima H, Riedy MC, Roberts JL, Aman MJ, Migone TS, Noguchi M, Markert ML, Buckley RH, O'Shea JJ, Leonard WJ. Mutation of Jak3 in a patient with SCID: essential role of Jak3 in lymphoid development. *Science* 1995; **270**: 797-800 [PMID: 7481768 DOI: 10.1126/science.270.5237.797]

81 **Leonard WJ**, Lin JX, O'Shea JJ. The γ_c Family of Cytokines: Basic Biology to Therapeutic Ramifications. *Immunity* 2019; **50**: 832-850 [PMID: 30995502 DOI: 10.1016/j.immuni.2019.03.028]

82 **James C**, Ugo V, Le Couédic JP, Staerk J, Delhommeau F, Lacout C, Garçon L, Raslova H, Berger R, Bennaceur-Griscelli A, Villeval JL, Constantinescu SN, Casadevall N, Vainchenker W. A unique clonal JAK2 mutation leading to constitutive signalling causes polycythaemia vera. *Nature* 2005; **434**: 1144-1148 [PMID: 15793561 DOI: 10.1038/nature03546]

83 **Flex E**, Petrangeli V, Stella L, Chiaretti S, Hornakova T, Knoops L, Ariola C, Fodale V, Clappier E, Paoloni F, Martinelli S, Fragale A, Sanchez M, Tavolaro S, Messina M, Cazzaniga G, Camera A, Pizzolo G, Tornesello A, Vignetti M, Battistini A, Cavé H, Gelb BD, Renauld JC, Biondi A, Constantinescu SN, Foà R, Tartaglia M. Somatically acquired JAK1 mutations in adult acute lymphoblastic leukemia. *J Exp Med* 2008; **205**: 751-758 [PMID: 18362173 DOI: 10.1084/jem.20072182]

84 **Druker BJ**, Tamura S, Buchdunger E, Ohno S, Segal GM, Fanning S, Zimmermann J, Lydon NB. Effects of a selective inhibitor of the Abl tyrosine kinase on the growth of Bcr-Abl positive cells. *Nat Med* 1996; **2**: 561-566 [PMID: 8616716 DOI: 10.1038/nm0596-561]

85 **Ferguson FM**, Gray NS. Kinase inhibitors: the road ahead. *Nat Rev Drug Discov* 2018; **17**: 353-377

[PMID: 29545548 DOI: 10.1038/nrd.2018.21]

86 **Schwartz DM**, Kanno Y, Villarino A, Ward M, Gadina M, O'Shea JJ. JAK inhibition as a therapeutic strategy for immune and inflammatory diseases. *Nat Rev Drug Discov* 2017; **17**: 78 [PMID: 29282366 DOI: 10.1038/nrd.2017.267]

87 **Sonbol MB**, Firwana B, Zarzour A, Morad M, Rana V, Tiu RV. Comprehensive review of JAK inhibitors in myeloproliferative neoplasms. *Ther Adv Hematol* 2013; **4**: 15-35 [PMID: 23610611 DOI: 10.1177/2040620712461047]

88 **Dhillon S**. Tofacitinib: A Review in Rheumatoid Arthritis. *Drugs* 2017; **77**: 1987-2001 [PMID: 29139090 DOI: 10.1007/s40265-017-0835-9]

89 **Al-Salama ZT**, Scott LJ. Baricitinib: A Review in Rheumatoid Arthritis. *Drugs* 2018; **78**: 761-772 [PMID: 29687421 DOI: 10.1007/s40265-018-0908-4]

90 **Taylor PC**. Clinical efficacy of launched JAK inhibitors in rheumatoid arthritis. *Rheumatology (Oxford)* 2019; **58**: i17-i26 [PMID: 30806707 DOI: 10.1093/rheumatology/key225]

91 **Papp K**, Gordon K, Thaçi D, Morita A, Gooderham M, Foley P, Girgis IG, Kundu S, Banerjee S. Phase 2 Trial of Selective Tyrosine Kinase 2 Inhibition in Psoriasis. *N Engl J Med* 2018; **379**: 1313-1321 [PMID: 30205746 DOI: 10.1056/NEJMoa1806382]

World Journal of Biological Chemistry

Submit a Manuscript: https://www.f6publishing.com

World J Biol Chem 2022 January 27; 13(1): 15-34

DOI: 10.4331/wjbc.v13.i1.15

ISSN 1949-8454 (online)

ORIGINAL ARTICLE

Basic Study

Increased monoamine oxidase activity and imidazoline binding sites in insulin-resistant adipocytes from obese Zucker rats

Christian Carpéné, Luc Marti, Nathalie Morin

ORCID number: Christian Carpéné 0000-0001-7765-6647; Luc Marti 0000-0002-8238-1147; Nathalie Morin 0000-0001-9793-371X.

Author contributions: Carpéné C designed the studies, performed hexose uptake assays and literature review, and wrote the manuscript; Marti L performed binding studies, rat experiments, and data analysis, and contributed to the literature review; Morin N performed immunoblots and data analysis, and revised the manuscript.

Institutional review board statement: The study was reviewed and approved by the Institutional Review Board of Institut des Maladies Métaboliques et Cardiovasculaires, Toulouse, France.

Institutional animal care and use committee statement: Rats were housed and manipulated according to the INSERM guidelines and European Directive 2010/63/UE by competent and expert technicians or researchers in animal care facilities with agreements number A 31 555 04 to C 31 555 011. The experimental protocol was approved by the local ethical committee CEEA nb122.

Conflict-of-interest statement: All

Christian Carpéné, Luc Marti, Nathalie Morin, Institut des Maladies Métaboliques et Cardiovasculaires, INSERM, Toulouse 31342, France

Nathalie Morin, Faculté de Pharmacie de Paris, Paris University, Paris 75270, France

Corresponding author: Christian Carpéné, PhD, Senior Researcher, Institut des Maladies Métaboliques et Cardiovasculaires, INSERM, CHU Rangueil, Bat. L4, BP 84225, Toulouse 31342, France. christian.carpene@inserm.fr

Abstract

BACKGROUND

Despite overt insulin resistance, adipocytes of genetically obese Zucker rats accumulate the excess of calorie intake in the form of lipids.

AIM

To investigate whether factors can replace or reinforce insulin lipogenic action by exploring glucose uptake activation by hydrogen peroxide, since it is produced by monoamine oxidase (MAO) and semicarbazide-sensitive amine oxidase (SSAO) in adipocytes.

METHODS

^{3}H-2-deoxyglucose uptake (2-DG) was determined in adipocytes from obese and lean rats in response to insulin or MAO and SSAO substrates such as tyramine and benzylamine. ^{14}C-tyramine oxidation and binding of imidazolinic radioligands [^{3}H-Idazoxan, ^{3}H-(2-benzofuranyl)-2-imidazoline] were studied in adipocytes, the liver, and muscle. The influence of *in vivo* administration of tyramine + vanadium on glucose handling was assessed in lean and obese rats.

RESULTS

2-DG uptake and lipogenesis stimulation by insulin were dampened in adipocytes from obese rats, when compared to their lean littermates. Tyramine and benzylamine activation of hexose uptake was vanadate-dependent and was also limited, while MAO was increased and SSAO decreased. These changes were adipocyte-specific and accompanied by a greater number of imidazoline I_2 binding sites in the obese rat, when compared to the lean. *In vitro*, tyramine precluded the binding to I_2 sites, while *in vivo*, its administration together with vanadium lowered fasting plasma levels of glucose and triacylglycerols in obese rats.

authors declare no competing financial interests for this article.

Data sharing statement: No additional data are available.

ARRIVE guidelines statement: The authors have read the ARRIVE guidelines, and the manuscript was prepared and revised according to the ARRIVE guidelines.

Supported by Recurrent Grants from Institut National de la Santé et de la Recherche Médicale to the INSERM U1048.

Country/Territory of origin: France

Specialty type: Endocrinology and metabolism

Provenance and peer review: Invited article; Externally peer reviewed.

Peer-review model: Single blind

Peer-review report's scientific quality classification

Grade A (Excellent): 0
Grade B (Very good): 0
Grade C (Good): C
Grade D (Fair): 0
Grade E (Poor): 0

Received: March 26, 2021
Peer-review started: March 26, 2021
First decision: July 8, 2021
Revised: July 9, 2021
Accepted: January 13, 2022
Article in press: January 13, 2022
Published online: January 27, 2022

CONCLUSION

The adipocytes from obese Zucker rats exhibit increased MAO activity and imidazoline binding site number. However, probably as a consequence of SSAO down-regulation, the glucose transport stimulation by tyramine is decreased as much as that of insulin in these insulin-resistant adipocytes. The adipocyte amine oxidases deserve more studies with respect to their putative contribution to the management of glucose and lipid handling.

Key Words: Obesity; Adipocyte; Amine oxidases; Imidazoline binding sites; Creatine kinase B; Idazoxan; Lipogenesis; Hydrogen peroxide; Glucose uptake

Core Tip: The substrates of monoamine oxidase (MAO) and semicarbazide-sensitive amine oxidase (SSAO) partly reproduce the stimulatory effect of insulin on sugar entry in rat fat cells. Especially when combined with vanadium, tyramine and benzylamine mimic more than 70% of the insulin stimulation of glucose uptake. Unfortunately, such insulin activation of glucose utilization is strongly diminished in the genetically obese Zucker rat, an animal model of the metabolic syndrome. In this insulin-resistant and obese rat, the stimulation of glucose transport by tyramine is decreased as much as that of insulin, while the effect of benzylamine is even more altered. SSAO, responsible for benzylamine oxidation, is down-regulated in adipocytes from obese Zucker rats. In contrast, MAO, which predominantly supports the oxidation of tyramine, is increased, apparently not in a sufficient manner to reach the same hexose uptake activation seen in fat cells from lean rats. However, this greater ability to oxidize tyramine was found only in white adipocytes from obese rats since no change was found in the liver or skeletal muscle when compared to lean controls. Moreover, increased MAO activity in the large adipocytes of obese rats was accompanied by an enlarged number of imidazoline binding sites, previously described to be located on MAO. Since the repeated subcutaneous administration of tyramine plus vanadate is somewhat capable of reducing plasma glucose and triglycerides in obese rats, SSAO, MAO, and its associated imidazoline I_2 sites deserve further studies with respect to their mimicking insulin action on glucose and lipid metabolism in fat cells.

Citation: Carpéné C, Marti L, Morin N. Increased monoamine oxidase activity and imidazoline binding sites in insulin-resistant adipocytes from obese Zucker rats. *World J Biol Chem* 2022; 13(1): 15-34
URL: https://www.wjgnet.com/1949-8454/full/v13/i1/15.htm
DOI: https://dx.doi.org/10.4331/wjbc.v13.i1.15

INTRODUCTION

Alongside the numerous models of transgenic mice exhibiting an overt obese phenotype, the Zucker fatty rat remains since decades one of the most widely studied animal models of genetic obesity. Obesity in these rats is inherited as an autosomal recessive trait, as initially reported in 1961 by Zucker and Zucker[1]. It was in 1996 that independent studies demonstrated the molecular basis of such obesity, which does not need any challenge with hypercaloric diet to develop spontaneously[2-4]. Affected rats have a missense mutation in the leptin receptor and show hyperphagia together with various endocrine and metabolic alterations similar to those that appear in the human metabolic syndrome. Leptin is an adipokine produced by adipose tissue and it plays an important role in the central regulation of energy balance[5], together with other functions (*e.g.*, in reproduction). Leptin activates its own receptors in the brain, thereby decreasing energy intake and increasing energy expenditure. Thus, the obese Zucker rats (previously called recessive homozygous fa/fa fatty rats) spontaneously exhibit bulimia and obesity and rapidly become hyperinsulinemic. Consequently, they have been considered as a useful model of insulin resistance and of dyslipidemia with related kidney diseases[6]. Nevertheless, the usefulness of Zucker fatty rats as a model of type 2 diabetes is questionable, since these hyperphagic animals have only mild

P-Reviewer: Yi X
S-Editor: Zhang H
L-Editor: Wang TQ
P-Editor: Zhang H

glucose intolerance, at the expense of dramatically increased insulin release by endocrine pancreas. Indeed, it has been reported that, during the early onset of obesity, the Zucker fatty rats are hypersensitive to insulin[7] and more capable to store lipids than their lean littermates[8]. One assumes that, once adult and obese, these rats develop alternative pathways allowing a still efficient storage of ingested energy in the form of triacylglycerols in the large lipid droplets of their adipocytes[9]. The impressive adipogenic and lipogenic activities maintained throughout the growth of fatty rats, boosted by an excessive energy intake, explains how 40% of body weight is composed of lipids when the Zucker rats reach 14 wk of age[9]. As in obese patients, the adipose depots of mature obese rats are hypertrophied despite established insulin resistance, which results in a lowered sensitivity of the adipocytes to anabolic actions of insulin such as lipogenesis stimulation[10]. The obese Zucker rat is, by definition, also resistant to leptin, and the obese animals present higher circulating levels of this adipokine compared to their lean littermate[11]. Our primary objective was to detect what type of adaptation might occur in adipocytes to circumvent such insulin/leptin resistance in order to maintain a still efficient fat deposition.

It has been reported that pharmacological adrenergic intervention on obese Zucker rats, such as treatment with the β-adrenergic agents celiprolol or clenbuterol[12,13], mitigates their insulin resistance, probably by improving insulin-stimulated glucose uptake in skeletal muscles and adipose tissues. The improvements were not accompanied with a notable body weight loss but were related to a tendency to normalize the repartition of energy fluxes between fat and muscular tissues[14]. To support such beneficial effect of reinforcing adrenergic inputs in the obese Zucker rat, was the demonstration that, in the adipose tissue of young suckling littermates, there was already, at 2 wk of age, a difference in the β-adrenergic signaling pathway in white adipocytes between the future obese and the future lean[15]. It is therefore admitted that impairment of the responsiveness to catecholamines plays a role in worsening the obesity syndrome triggered by leptinergic system invalidation. This led us to further study the alterations of biogenic amine pathways in obese Zucker rats, since these metabolites have a potential role as biomarkers of the metabolic syndrome [16].

It has been already reported that the basal lipolytic activity is higher in adipocytes from obese rats, and that resistance to the lipolytic action of catecholamines appears to counteract such elevated baseline lipolysis[17]. This decrease of β-adrenergic responsiveness seems therefore to be an adaptive mechanism aiming at moderating *in vivo* increase in plasma free fatty acids (FFA). In fact, any excessive increase in circulating FFA is deleterious as it contributes to the complications of insulin-resistant states, such as hepatic steatosis. In addition to their important role in lipid mobilization, the catecholamines also activate glucose utilization in muscles[18] and in brown adipose tissue (BAT)[19]. In a recent study, we observed that high doses of catecholamines mimic the stimulatory effects of insulin on glucose transport, at least *in vitro* in rodent isolated adipocytes[20]. All these observations indicated that amines might constitute factors other than insulin capable of affecting directly glucose utilization in fat cells. More precisely, the insulin-like effect of high doses of catecholamines was independent from adrenoceptor stimulation and was rather depending on the presence of the tyrosine phosphatase inhibitor vanadium[20]. In this complex situation, we focused our comparison between lean and obese Zucker rats on the still elusive influence of amines on adipose cell biology.

Alongside their activation of receptors on pre- and post-synaptic cell types, catecholamines are exquisitely regulating various adipocyte functions, *via* their rapid release from presynaptic vesicles or other supposed stores[21,22] and their prompt turn-off mechanisms, involving reuptake, degradation, and desensitization to avoid overstimulation. One of the major catabolic steps of catecholamine degradation is catalyzed by monoamine oxidase (MAO). When oxidating any given substrate, MAO does not only terminate its neurotransmitter function, it also releases the corresponding aldehyde and hydrogen peroxide. The MAO activity has been reported to be lower in the liver of the obese than in the lean rat[23], but to our knowledge, no report has described so far a change of this mitochondrial enzyme in adipose depots.

The following results will compare in obese and lean Zucker littermates, the metabolic effects of a MAO substrate, tyramine, as well as its oxidation by MAO and another amine oxidase highly expressed in fat cells, the semicarbazide-sensitive amine oxidase (SSAO). The data presented thereafter will also indicate that the imidazoline binding sites (I_2-sites) that have been documented to be present on MAO[24-27] are more numerous in the white adipose tissue (WAT) of the obese than in the lean rat.

MATERIALS AND METHODS

Chemicals

2-1, 2-^{3}H-deoxy-D-glucose (2-DG; 10 Ci/mmol), 3-^{3}H-D-glucose (10 Ci/mmol), and ^{14}C-tyramine were from PerkinElmer (Shelton, United States). ^{3}H-2-(2-benzofuranyl)-2-imidazoline (^{3}H-BFI; 50 Ci/mmol) and ^{3}H-Idazoxan (42 Ci/mmol) were purchased from Amersham Bioscience/GE Healthcare in 2004 (Buckinghamshire, England), then isotopically diluted in ethanol and stored at -12 °C, and yearly verified since by high performance liquid chromatography (> 90% pure) before being used as radioligands for binding experiments until 2010. Electrophoresis products and devices were from Bio-Rad (Ivry/Seine, France). Rabbit polyclonal antibodies against MAO and SSAO were kindly given by Pr. A. Parini (Toulouse, France), and by Pr. M. Unzeta (Barcelona, Spain), respectively. Rauwolscine was kindly given by Dr. A. Remaury (Sanofi, Chilly-Mazarin, France). All remaining chemicals and drugs, such as cirazoline, sodium orthovanadate, and bovine insulin, were purchased from Merck (Darmstadt, Germany) or its affiliate Sigma-Aldrich (Paris, France).

Animals

Three sets of experiments were successively performed to explore the imidazoline binding sites and the MAO/SSAO activities in various tissues from Zucker rats, and the functional response of adipocytes. All the comparisons between lean and obese Zucker rats were made between littermates. Such comparative approach between littermates was performed on a number of male and female rats that was not always the same for each genotype in each successive experiment. This was due to the fact that the number of pups of a given litter is not always distributed equally according to the gender and to the obese phenotype (which were stated after weaning only). Consequently, the number and gender of analyzed animals are given thereafter for each subset of experiments. All the rats (Charles River Laboratories, L'Arbresle, France) were housed in hanging wire cages with free access to food and water on a 12 h light/dark cycle (lights on 6 a.m.) at a temperature of 20 °C. They were euthanized after overnight fasting between 9 and 10 wk of age in accordance with the ARRIVE guidelines (Animal Research: Reporting of *In Vivo* Experiments)[28].

Adipocyte glucose uptake and lipogenic activity

WAT was removed from intra-abdominal (perigonadic, retroperitoneal, and perirenal; thereafter named visceral WAT) and from subcutaneous (inguinal) locations. It was immediately digested by collagenase in Krebs-Ringer buffer containing 15 mmol/L bicarbonate, 10 mmol/L HEPES, 2 mmol/L pyruvate, and 3.5% bovine serum albumin. Separation, washing, and dilution of the buoyant adipocytes were performed in the immediate continuity at 37 °C with fresh buffer prior to the functional assays, which were performed as previously described[20].

The radiolabeled non-metabolizable analog of glucose, ^{3}H-2-DG, was used at 0.1 mmol/L for hexose uptake assays as described previously[20], save that the assays lasted 5 min instead of 10 min for human fat cells, which are less metabolically active.

Lipogenic activity was determined by measuring the radioactivity incorporated into cellular lipids after 120-min incubation with the indicated agents and 0.5 mmol/L ^{3}H-glucose. This very simple bioassay, primarily designed by Moody and coworkers[29], was performed with slight adaptations[30] in the same plastic vial, which was used for incubation, extraction, and scintillation counting, since the ^{3}H-glucose that was not metabolized by the fat cells remained in the lower phase and could not excite the non-water-miscible liquid scintillation cocktail (InstaFluor-Plus, PerkinElmer, Waltham, United States) of the upper phase, containing the neosynthesized lipids, as already demonstrated[31].

Immunoblots

Homogenates were prepared in RIPA buffer, and proteins were solubilized in loading buffer (60 mmol/L Tris-HCl with 2% SDS, 10% glycerol, 1% β-mercaptoethanol, pH 6.8) at 100 °C for 5 min prior to sodium dodecyl sulfate-polyacrylamide gel electrophoresis. After migration, proteins were transferred to polyvinylidene difluoride membranes with a semidry electroblotter (Trans-blot, Bio-Rad). The blots were blocked in wash buffer (50 mmol/L Tris, 200 mmol/L NaCl, 0.1% Tween 20, pH 7.5) with 5% nonfat dried milk for 1 h at room temperature. Then they were incubated overnight at 4 °C with rabbit polyclonal antisera (1:1000) obtained from rabbits immunized against an epitope of MAO-A and MAO-B as described previously[32]. After washing, the blots were incubated with peroxidase-labeled anti-rabbit IgG

(1:7000) in wash buffer for 60 min. The immunoreactive proteins were detected using enhanced chemiluminescence (Pharmacia Biotech, Piscataway, NJ). Similar procedure was followed when using an anti-SSAO polyclonal antibody developed and tested previously[33]. β-actin amount was determined in stripped membranes, and as no change was observed between preparations from lean and obese animals (not shown), no normalization to β-actin was performed.

Amine oxidase assay

Amine oxidase activity was measured on homogenates of thawed tissues with ^{14}C-tyramine in 200 mM phosphate buffer in the presence of an antiprotease cocktail from Sigma as previously described[30]. MAO activity was defined as oxidation inhibited by pargyline 0.1 mmol/L, while SSAO activity was sensitive to semicarbazide 1 mmol/L. BAT was removed from the core of the interscapular fat depot, and the soleus muscle was chosen as representative of skeletal muscles. Like liver samples, these tissues were snap-frozen without buffer and homogenates were prepared on thawed samples as already described[34]. Protein content was measured with DC-protein assay from Bio-Rad. In the case of amine oxidation by intact fat cells, 1 mM of an isotopic dilution of ^{14}C-tyramine was incubated for 30 min with adipocyte suspension (~10 mg of cell lipids) in 400 µl of KRBH medium instead of phosphate buffer, and treated as above stated for homogenates.

Radioligand binding

For saturation-binding isotherms, membranes were incubated with increasing concentrations of ^{3}H-idazoxan at room temperature for 45 min in Tris-HCl buffer, pH 7.4. The presence of 10 µmol/L rauwolscine was used to mask α_2-adrenoceptors as already demonstrated[32]. For ^{3}H-BFI, it was not necessary to preclude binding to adrenergic receptors since this imidazolinic radioligand has been shown to be selective for the I_2-sites[30,35,36]. In both cases, incubation was stopped by vacuum filtration through Whatman GF/C microfilters with extensive washes with the same buffer at 4 °C. Nonspecific binding was defined in the presence of 100 µmol/L cirazoline and represented 30% to 50% of the total binding depending on the radioligand nature, its concentration, and the biological material tested. Radioactivity bound on the filters was counted in a liquid scintillation spectrometer (Packard, model Tri-Carb 4000) with 4 mL of Packard Emulsifier-Safe scintillation fluid per scintillation microvial.

Statistical analysis

Results are presented as the mean ± SEM of (*n*) observations. Statistical analyses for comparisons between parameters were performed using ANOVA followed by post-hoc Dunnett's multiple comparisons test, and were performed with Prism 6 for Mac OS X (from GraphPad software, San Diego, CA).

RESULTS

Hyperinsulinemia and insulin resistance of adipocytes are characteristic traits of the obese Zucker rat

Some characteristic features of the obese Zucker rats were first verified. At the age of 9-10 wk, the obese rats exhibited larger body weight and adiposity, with elevated insulin and triacylglycerol plasma levels, when compared to their lean littermates of the same age (Table 1). Fasting plasma glucose levels were slightly higher in the obese group, but with a less pronounced difference with respect to the other circulating parameters influenced by genotype. Blood glucose was 1.12 times higher in obese rats, while insulin was four to five times higher and triacylglycerol two times higher than in lean controls. As expected, the males bearing the two alleles with the mutated leptin receptor (fa/fa) were hyperphagic since their daily food consumption was increased by 1.3 times, *i.e.*, similarly to their increased body weight, while the sum of their dissected fat depots was five-to-six-fold heavier than in lean littermates (Table 1).

Our descriptive approach readily confirmed in white adipocytes the insulin-resistant state of the obese rats, which accompanies their clear-cut hyperinsulinemia. The hexose uptake assays showed that the maximal effect of insulin (obtained at 0.1 µmol/L-1 µmol/L) was one-half lower in obese than in lean rats (Figure 1A). The white adipocytes of obese rats also exhibited a reduced sensitivity to insulin: Their response to 10 nmol/L insulin represented less than 60% of the maximal effect of the pancreatic hormone in obese rats while it reached 80% in lean controls (Figure 1A). A

Table 1 Biological parameters of the lean and obese rats used in this study

Littermate phenotype	Lean (8)	Obese (9)
Final body weight (g at 9-10 wk)	230 ± 21	312 ± 16[b]
Visceral WAT weight (g)	1.8 ± 0.3	8.9 ± 1.4[c]
Subcutaneous WAT weight (g)	2.5 ± 0.3	13.4 ± 1.6[c]
Plasma levels		
Insulin (UI/mL)	37 ± 2	178 ± 46[b]
Glucose (mmol/L)	7.7 ± 0.2	8.6 ± 0.2[a]
Triacylglycerols (mmol/L)	0.7 ± 0.2	1.5 ± 0.1[b]

Significantly different from each corresponding value in lean at:
[a]$P < 0.05$.
[b]$P < 0.01$.
[c]$P < 0.001$.
mean ± SEM of the number of rats indicated in parentheses.

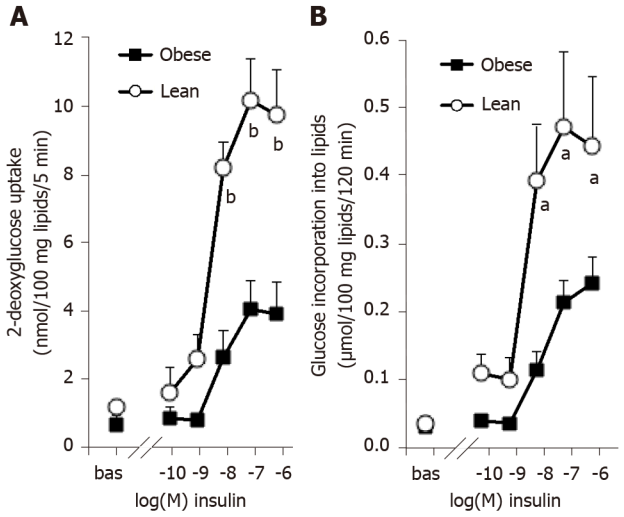

Figure 1 Influence of obesity on the dose-dependent responses of rat adipocytes to insulin activation of hexose uptake and of lipogenesis. A: ^{3}H-2-deoxyglucose (2-DG) transport was assayed for 5 min after 45-min incubation of rat fat cells without (bas) or with increasing doses of insulin. 2-DG uptake is expressed as nmoles of intracellular radiolabeled 2-DG/100 mg lipids/5 min; B: ^{3}H-glucose incorporation into lipids was measured after 120-min incubation with the indicated doses of insulin and is expressed as µmoles tritiated glucose incorporated/100 mg lipids. Adipocytes from lean (open circles) or obese rats (black squares) were incubated at a cell suspension averaging 11.5 and 11.7 mg lipids/assay tube, respectively. A significant influence of genotype on the three higher doses of insulin was found at [b]$P < 0.001$ for 2-DG uptake (n = 10 lean and 10 obese male rats, with male/female = 1) and at [a]$P < 0.05$ for lipogenesis (n = 8 lean and 6 obese male rats). Each point is the mean ± SEM of n animals, with error bars lying within the caption in several occurrences.

similar pattern was obtained when lipogenic activity of the adipocytes was assessed by the incorporation of radioactivity into cell lipids after 120-min incubation with 3-^{3}H-D-glucose (Figure 1B). The insulin resistance was not totally complete in these young obese rats, since the baseline incorporation was increased by a six-fold factor in response to 100 nmol/L insulin. Nevertheless, this maximal activation reached a 12-fold factor in adipocytes from lean rats (Figure 1B). As for hexose transport, the lipogenic effect of 10 nmol/L insulin reached 42% ± 8% and 86% ± 7% of maximal response in obese and lean rats, respectively (n = 8 and 6, respectively, $P < 0.002$).

In order to bring evidence that other factors other than insulin may help the adipocytes in accumulating large amounts of lipids during the growth of the insulin-resistant obese rat, vanadium was tested alone and with hydrogen peroxide, either when directly added at 1 mmol/L, or when generated endogenously by the adipocytes *via* the oxidation of the MAO and SSAO substrates tyramine and benzylamine at 1 mmol/L (Figure 2). Sodium orthovanadate was inefficient at 100 µmol/L, either on basal or on insulin-stimulated 2-DG uptake. However, vanadium potentiated the insulin-mimicking action of 1 mmol/L hydrogen peroxide. The combination of these

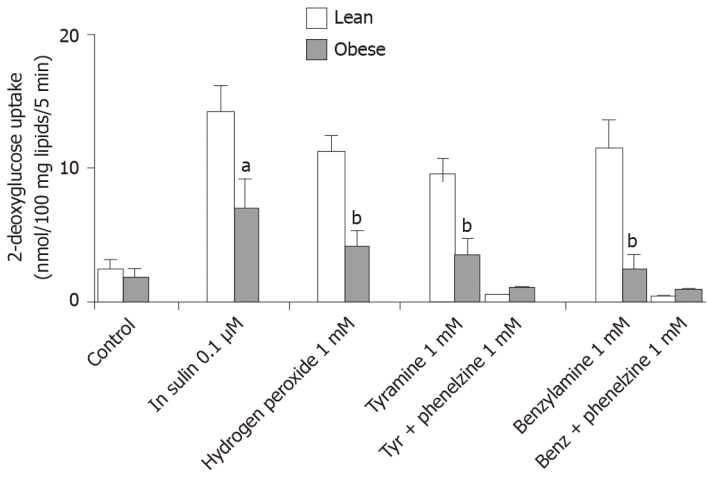

Figure 2 Insulin-like effects of vanadium combined with hydrogen peroxide or with amine oxidase substrates on hexose uptake into rat adipocytes. Sodium orthovanadate was present at 100 µmol/L in all the conditions: Alone (control) or combined with 100 nmol/L insulin, or with 1 mmol/L hydrogen peroxide, tyramine, and benzylamine. The amines were tested without and with 1 mmol/L phenelzine. 2-deoxyglucose (2-DG) uptake is expressed as nmoles of intracellular 2-DG/100 mg lipids/5 min. Mean ± SEM of five lean (open columns) and five obese male rats (shaded columns). Significantly different from corresponding condition in lean at: $^{a}P < 0.05$; $^{b}P < 0.01$. Blockade of tyramine (tyr) or benzylamine (benz) effect by phenelzine was significant at $P < 0.001$ in both genotypes.

two agents is known to generate peroxovanadate, a powerful protein tyrosine phosphatase inhibitor[37,38]. It led to a stimulation of glucose uptake equivalent to 70%-80% of the response to insulin in lean rats (Figure 2). Tyramine, a substrate of both MAO and SSAO in rodents[34], was also able, when combined with vanadium, to reproduce 60%-70% of insulin maximal response in the lean rats. This insulin mimicry was also obtained with 1 mmol/L benzylamine, but it represented 84% ± 16% of insulin + vanadate effect in lean and only 38% ± 7% in obese rats ($n = 5$, $P < 0.03$). As expected, the MAO and SSAO inhibitor phenelzine abolished the effects of tyramine or benzylamine plus vanadium in both genotypes (Figure 2).

These first observations indicated that the MAO- or SSAO-mediated effects of tyramine on glucose handling by fat cells were limited similarly as those of insulin in obese Zucker rats. However, since the effect of benzylamine plus vanadate seemed to decrease even more with obesity, we further studied the protein expression of the amine oxidases in WAT.

Western blot analysis of amine oxidases in adipose tissues of lean and obese Zucker rats

When the expression of MAO and SSAO was determined by Western blot in subcutaneous WAT, opposite changes were observed for these membrane proteins. WAT expressed less SSAO in obese than in lean rats, at least in the subcutaneous depots of 10-wk-old animals (Figure 3). This lower abundancy was agreeing with the above reported lower insulin-like effects of benzyamine regarding glucose uptake in adipocytes. More puzzling was the obesity-related increase in MAO-A protein, while MAO-B was poorly affected in obese rats. As a consequence of these opposite regulations, the resulting effect on glucose transport of the MAO and SSAO substrate tyramine did not exhibit a dramatic change in adipocytes from obese rats, at least when normalized to the maximal insulin response. To state whether tyramine catabolism is really greater in WAT from obese rats, it was decided to investigate its oxidation in various tissues.

Amine oxidase activities in several tissues of lean and obese Zucker rats

The oxidation of 0.5 mmol/L ^{14}C-tyramine by crude membranes of different tissues is shown in Figure 4, in which 'total oxidation' means spontaneous oxidation of the amine in the presence of biological material, without any added inhibitor or catalyst. Since the liver is known for being rich in MAO activity, it was tested here as a positive control. As expected, the liver was the richest of the tested tissues regarding MAO activity, which entirely supported total tyramine oxidation, and which did not exhibit difference between genotypes. No SSAO activity was detectable in liver homogenates regardless of the genotype.

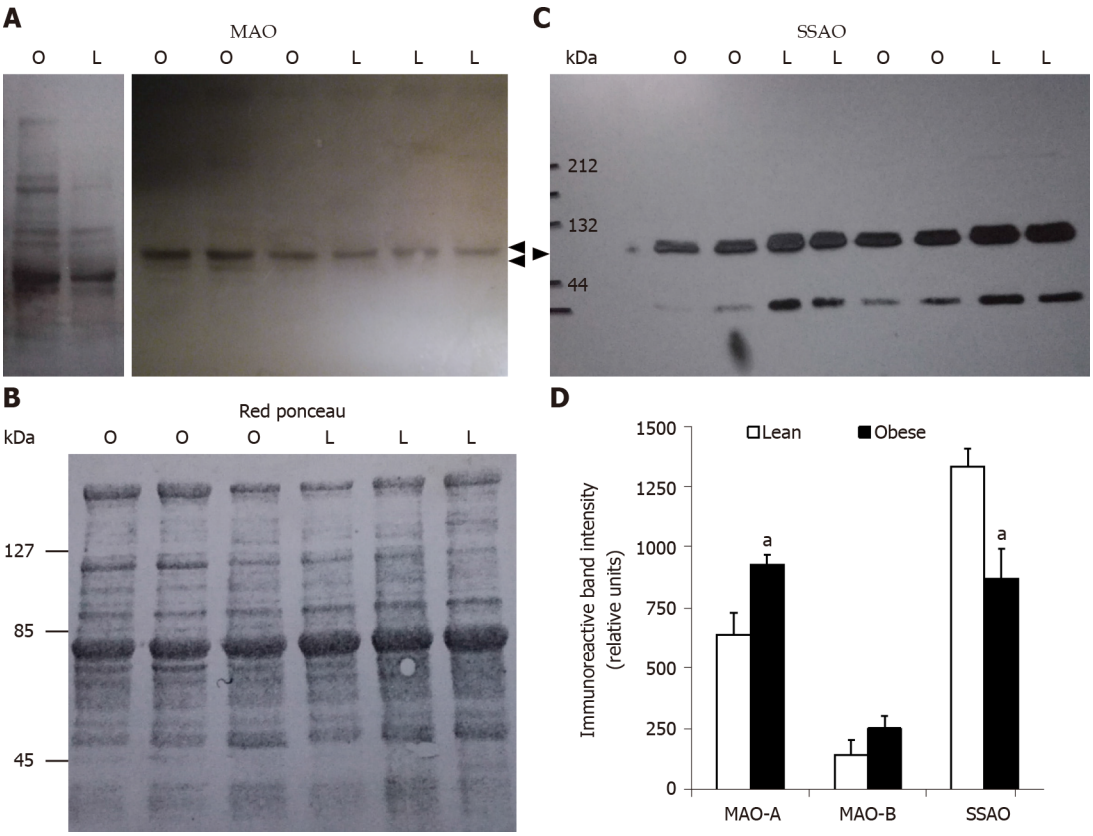

Figure 3 Increased monoamine oxidase and decreased semicarbazide-sensitive amine oxidase protein expression in subcutaneous adipose tissue from obese rats when compared to lean littermates. Proteins solubilized from white adipose tissue homogenates were separated by sodium dodecyl sulfate-polyacrylamide gel electrophoresis and blotted proteins detected using primary antibodies directed against monoamine oxidase (MAO) or semicarbazide-sensitive amine oxidase (SSAO). 50 μg and 5 μg proteins per lane were deposed for MAO and SSAO immunoblots, respectively. A: Immunoblots showing immunoreactive MAO-A and MAO-B at approximately 61 and 55 kDa (arrows) for obese (O) and lean (L) rats; B: Red ponceau control of protein loading for a representative membrane shown in panel A; C: Representative immunoblot of SSAO showing a major band at approximately 85 kDa (arrow); D: Densitometry analysis of the major bands is shown for 7-8 rats per genotype. Different from lean (open columns) at: $^{a}P < 0.05$.

Tyramine oxidation in crude membranes of adipose cells from visceral fat depots was greater in obese than in lean rats (Figure 4). This was largely due to an increased MAO activity, which was prominent in white adipocytes when considering the large proportion of total tyramine oxidation that was inhibited by pargyline (therefore MAO-dependent). The smaller fraction of tyramine oxidation that was sensitive to semicarbazide (therefore SSAO-dependent) was not clearly reduced in visceral adipocytes from obese rats (Figure 4). Altogether, these changes were similar to those observed in immunoblots of subcutaneous WAT.

In the interscapular adipose tissue, which contains brown adipocytes, thereby considered as BAT, increased tyramine oxidation was also found in obese rats (Figure 4). Although both MAO and SSAO activities were higher in BAT from obese than from lean rats, none of them reached the levels found in WAT. Lastly, in skeletal muscle crude membranes, tyramine oxidation was weak regardless of the genotype.

The fact that an increase in tyramine oxidation only occurred in WAT and BAT raised a concern about possible yield variations during membrane preparation between obese and lean rats. In fact, only the adipose depots were impressively much fatter in the obese than in the lean rat, while this was less evident for the liver and skeletal muscles. To circumvent a possible bias generated by an excess of fat in the different centrifugation steps necessary for membrane preparation, we studied the genotype influence on the capacity to oxidize tyramine in undamaged, functional adipocytes freshly isolated from visceral WAT. Again, adipocytes from obese rats possessed a higher capacity to oxidize tyramine when compared to lean ones (Figure 5). Even being of larger cell size, the adipocytes of obese Zucker rats definitely exhibited a larger MAO activity than lean controls. Figure 5 also shows that the same SSAO activity was found in adipocytes from obese rats and lean controls. Finally, MAO and SSAO activities were complementary to account for the total tyramine oxidation performed by adipocytes, ruling out a notable contribution of other amine oxidases.

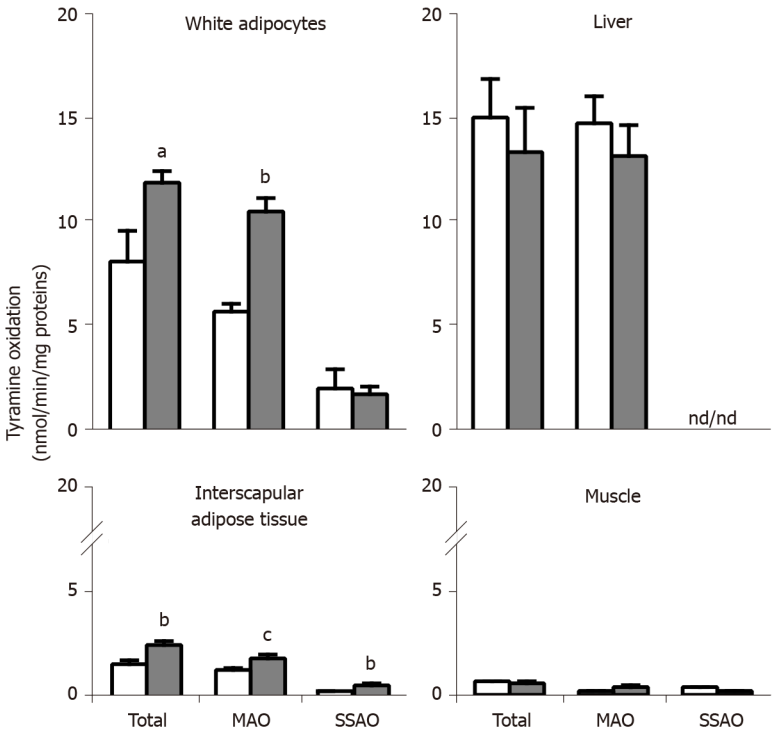

Figure 4 Oxidation of tyramine by membrane preparations from different tissues of obese and lean Zucker rats. Crude membranes prepared by centrifugation from adipocytes isolated from visceral white adipose tissue, or from the liver, brown adipose tissue, and soleus muscle, were incubated for 20 min at 37 °C with 0.5 mmol/L ^{14}C-tyramine in phosphate buffer (200 mmol/L) without (total oxidation), with 1 mmol/L semicarbazide (monoamine oxidase, MAO), or with 1 mmol/L pargyline (semicarbazide-sensitive amine oxidase, SSAO). The minor oxidation remaining in the presence of both inhibitors (semicarbazide + pargyline), therefore non-SSAO and non-MAO, was subtracted in all cases. Mean ± SEM from four determinations for lean (open columns) and five for obese male rats (dark columns); ND: Non-detectable. Significantly different from lean at: $^{a}P < 0.05$; $^{b}P < 0.01$; $^{c}P < 0.001$.

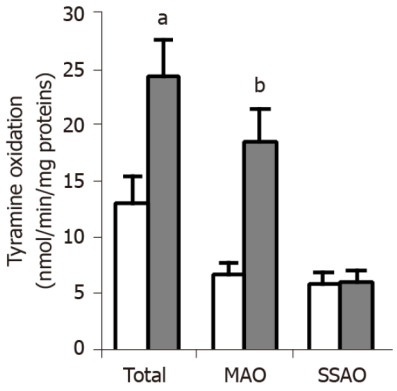

Figure 5 Tyramine oxidation in adipocytes from obese and lean Zucker rats. Undamaged adipocytes isolated from visceral white adipose tissue of lean (open columns) and obese (dark columns) rats were incubated in the presence of 1 mmol/L ^{14}C-tyramine for 45 min at 37 °C. Total oxidation was measured without any inhibitor, while the oxidation that resisted to 1 mmol/L semicarbazide was due to monoamine oxidase, and the oxidation resistant to 1 mmol/L pargyline was semicarbazide-sensitive amine oxidase-dependent. The velocities of oxidation are expressed as as nmoles of radiolabeled tyramine oxidation products generated per min and per mg of proteins. Each column is the mean ± SEM of eight determinations for lean and nine determinations for obese male rats. Significantly different from lean at: $^{a}P < 0.05$; $^{b}P < 0.01$.

In view of the enlarged MAO activity that appeared specific for WAT and BAT, we reanalyzed in various tissues from obese and lean rats an unpublished comparison of the population of I_2 imidazoline binding sites, previously described to be present on MAO enzymes[24,26,27] and distinct from the I_1 sites, essentially labeled by clonidine or moxonidine[39,40].

Pharmacological analysis of imidazoline binding sites in tissues of lean and obese Zucker rats

By using a saturating concentration of ^{3}H-BFI (20 nmol/L), we quantified the I_2

imidazoline binding sites in crude membranes from the same anatomical locations as above. A difference in the amount of ^{3}H-BFI bound was evident between obese and lean rats in visceral adipocytes only. The obese rats exhibited the same ^{3}H-BFI binding as the lean controls in the liver, interscapular BAT, and skeletal muscle (Figure 6).

This comparison was completed by saturation binding experiments in adipocyte membranes from visceral and subcutaneous WAT with ^{3}H-BFI and ^{3}H-idazoxan. Increasing concentrations of ^{3}H-BFI (from 0.2 to 26 nmol/L) resulted in saturation curves for total binding, with a clearly lower non-specific binding that was defined in the presence of 100 µmol/L cirazoline (Figure 7). Scatchard plots of the resulting specific binding gave an almost linear relationship between the bound/free ratio and the quantity of bound radioligand (Figure 7). The estimates of the affinity constant (K_D) and of the population density (B_{max}) of the corresponding single class of binding sites are reported in Table 2. A significant increase of the number of I_2 imidazoline binding sites was found in WAT of the obese Zucker rats when compared to lean controls. The nature of these binding sites was not modified by the obesity status since the K_D values were not different between obese and lean rats (Figure 7 and Table 2).

Similar saturation binding parameters were observed when using ^{3}H-idazoxan (from 0.7 to 45 nmol/L) as radioligand in the presence of 10 µmol/L rauwolscine to preclude its binding to α_2-adrenoceptors. Again, higher B_{max} values were found in the WAT of obese rats without notable change in K_D values when compared to lean controls (Figure 7 and Table 2). ^{3}H-idazoxan exhibited a lower affinity for the I_2 sites than ^{3}H-BFI, and it exhibited also a less selectivity towards imidazoline sites since, at 14 nmol/L, non-specific binding reached 50% of total binding in lean while it represented 10% of total binding in obese rats (not shown).

Nevertheless, the B_{max} values obtained with ^{3}H-idazoxan were of the same order of magnitude as the values observed with ^{3}H-BFI, suggesting that both imidazolinic radioligands recognized the same binding sites. Moreover, the observed increase in the density of I_2 sites in obese rat could not be associated to changes in the protein amounts used in binding experiments since we used similar protein levels regardless of the genotype, at least for visceral WAT (Table 2).

Thus, the larger density of I_2 sites specifically found in the WAT of obese rats was related to an increased MAO activity. Binding data were also in agreement with the previously reported capacity of BFI to inhibit MAO activity present in human and rodent adipose tissues[30]. To further explore the functional link between I_2 sites, MAO activity, and tyramine insulin-like effect, we performed two distinct approaches, one consisting in a short-term *in vitro* experiment on the interplay between I_2 binding sites and MAO activity, and the other based on repeated *in vivo* administration of tyramine plus vanadate to Zucker rats.

Since MAO activity and I_2 binding sites appeared to be linked with respect to their higher levels in WAT from obese rats when compared to lean controls, we took advantage of their abundancy in the liver to verify whether the one can influence the other. Figure 8 shows the total and the non-specific binding of increasing doses of ^{3}H-idazoxan to liver crude membranes from lean Zucker rats. The former followed a curve reaching saturation while the latter was linearly increasing with radioligand concentration. Addition of a large dose of tyramine (5 mmol/L) to saturate the active sites of hepatic MAO abolished the total idazoxan binding without altering the non-specific one. This confirmed the functional interaction between MAO activity and I_2 binding sites.

In vivo treatment of lean and obese rats with tyramine plus vanadate

A repeated treatment with 'tyramine + vanadate' was performed on 9-wk-old lean and obese rats to investigate whether the *in vitro* insulin-mimicking effects of this combination could have any *in vivo* relevance. The subcutaneous administration of tyramine at 3 mg/kg/d combined with sodium orthovanadate at 0.3 mg/kg/d for 1 wk was well tolerated, and did not modify significantly the body weight gain in obese rats when compared to controls receiving the vehicle (daily s.c. bolus of 0.3 mL NaCl 0.9%): 47 + 8 *vs* 46 ± 8 g (n = 3-4, NS). Body weight gain was also unaltered in treated lean rats (33 ± 3 *vs* 32 ± 3 g; n = 3-4, NS). Daily food intake was also unchanged since it remained around 23 g/rat in the treated and control lean groups, and was comprised between 29 and 40 g/rat in the obese groups (not shown). Obviously, the clear-cut difference between obese and lean rats regarding fat deposition could not be modified by this relatively short-term treatment. Only a non-significant tendency to enhance the mass of dissected adipose depots was seen in obese treated rats, while one of the dissected fat depots was heavier in lean rats receiving tyramine (Figure 9). Interestingly, tyramine + vanadate treatment reduced moderately but significantly the fasting plasma levels of glucose and triacylglycerols in the obese treated group (Figure 9).

Table 2 Imidazoline binding sites labeled by ^{3}H-2-(2-benzofuranyl)-2-imidazoline or ^{3}H-idazoxan: Comparison between visceral and subcutaneous white adipose tissues of lean and obese rats

Radioligand genotype	^{3}H-BFI		^{3}H-idazoxan + rauwolscine 10 μmol/L	
	Lean	Obese	Lean	Obese
	Visceral WAT			
Bmax (fmol/mg protein)	608 ± 39	1467 ± 208[c]	232 ± 42	1268 ± 108[c]
K_D (nmol/L)	8.9 ± 2.0	6.5 ± 0.5	16.9 ± 2.2	17.6 ± 2.6
proteins (μg/assay)	45 ± 6	49 ± 2	34 ± 7	46 ± 2
	Subcutaneous WAT			
Bmax (fmol/mg protein)	309 ± 25	1046 ± 12[c]	212 ± 39	914 ± 53[c]
K_D (nmol/L)	9.3 ± 0.8	5.7 ± 1.2	22.5 ± 2.3	16.5 ± 3.1
proteins (μg/assay)	51 ± 7	83 ± 12[a]	51 ± 7	83 ± 12[a]

Significantly different from each corresponding value in lean at:
[a]$P < 0.05$.
[c]$P < 0.001$.
The maximal binding value, B_{max} expressed as fmol/mg proteins, and affinity constant, K_D expressed as nmol/L, were calculated from three independent Scatchard plots built for each radioligand. The mean quantity of membrane proteins used per assay tube is also reported for each white adipose tissue anatomical location and radioligand.

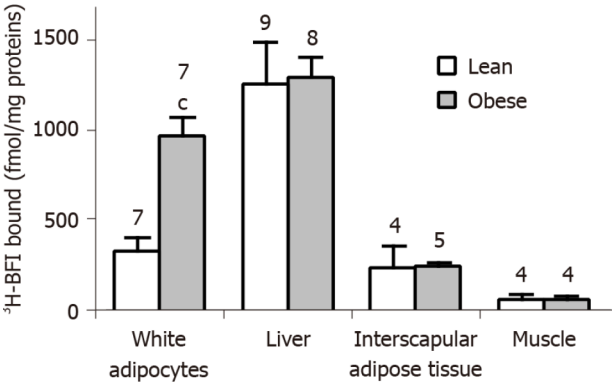

Figure 6 Tissue-selective larger imidazoline binding site density in the white adipocytes from obese rats when compared to lean littermates. Crude membranes were prepared from adipocytes isolated from white subcutaneous fat depots, the liver, interscapular brown adipose tissue, and soleus muscle, and incubated for 45 min with 20 nmol/L ^{3}H-2-(2-benzofuranyl)-2-imidazoline (^{3}H-BFI), before separation by vacuum filtration as indicated in Methods. Only the specific binding of ^{3}H-BFI, *i.e.*, displaceable by 100 μmol/L cirazoline, is shown. For each tissue, there was one determination of specific binding per rat, calculated by the difference between total and non-specific binding. Results are the mean ± SEM of the number of rats indicated above each column (open for lean, shaded for obese rats). Significantly different from corresponding value in lean at: [c]$P < 0.001$.

Regarding glucose uptake, the tyramine + vanadate treatment was not sufficient to mitigate the clear insulin-resistant state of the adipocytes of obese Zucker rats (Figure 9). However, it was investigated whether the insulin-effect of peroxovanadate on glucose transport in adipocytes (generated by *in vitro* addition of 1 mmol/L hydrogen peroxide + 0.1 mmol/L vanadate) was modified by the tyramine + vanadate treatment, especially in the obese rats, in view of their higher MAO content. The hexose uptake stimulated by hydrogen peroxide plus vanadate was similar in control and treated obese rats: 4.19 ± 1.30 and 3.29 ± 1.55 nmol 2-DG/100 mg lipids/5 min, respectively (n = 5, NS). Again, this peroxovanadate-dependent stimulation of hexose uptake was higher in lean rats, regardless of treatment: 11.32 ± 1.26 and 10.46 ± 2.61 nmol 2-DG/100 mg lipids/5 min (n = 5, NS). Nevertheless, it is worth noting that these values were, in each genotype, close to the maximal stimulation of hexose uptake triggered by high doses of insulin (see Figure 9). At least, the tyramine + vanadate treatment did not induce any desensitization of the insulin mimicking action of hydrogen peroxide plus vanadate.

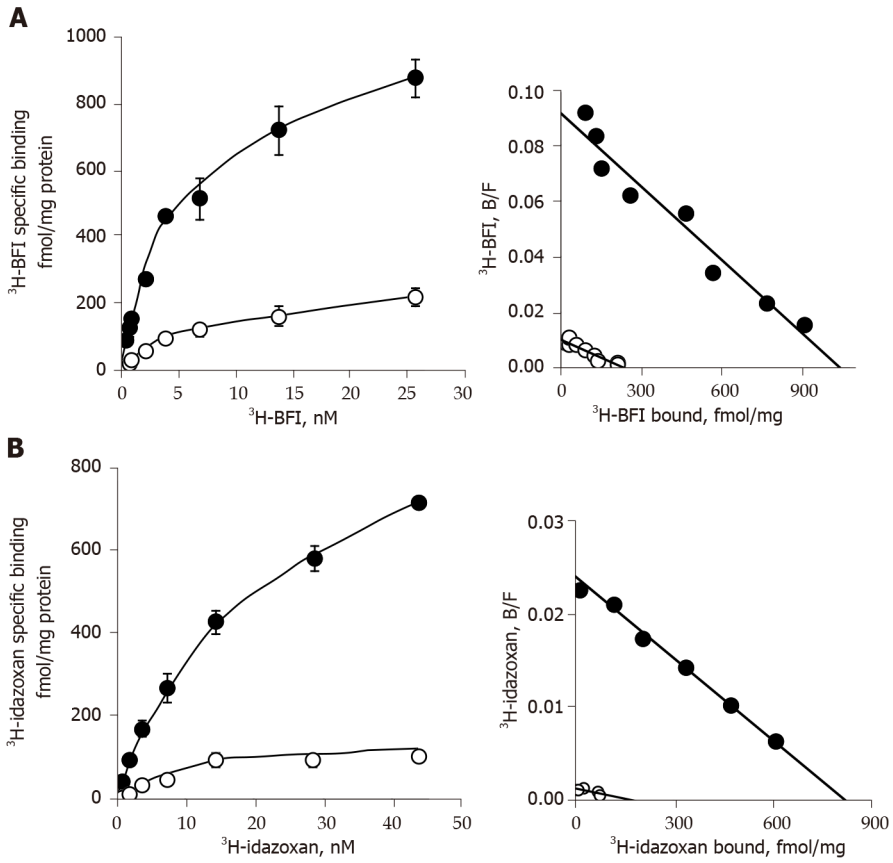

Figure 7 Saturation binding analysis with ^{3}H-2-(2-benzofuranyl)-2-imidazoline and ^{3}H-idazoxan in adipocyte membranes from white subcutaneous adipose tissue of lean and obese rats. A and B: Adipocyte membranes from subcutaneous white adipose tissue of lean (open circles) or obese (dark circles) littermates were incubated for 45 min with increasing concentrations of ^{3}H-2-(2-benzofuranyl)-2-imidazoline alone (A) or ^{3}H-idazoxan plus 10 μmol/L rauwolscine (B). For each tested concentration, total binding was measured in the absence of any competitor while non-specific binding was determined in the presence of 100 μmol/L cirazoline. Left panels show the saturation curves of specific binding, with each point corresponding to the mean ± SEM of three separate saturation experiments. Right panels show the Scatchard plot (bound/free *vs* bound) of the saturation experiment for each radioligand. Calculated parameters of saturation experiments are reported in Table 2.

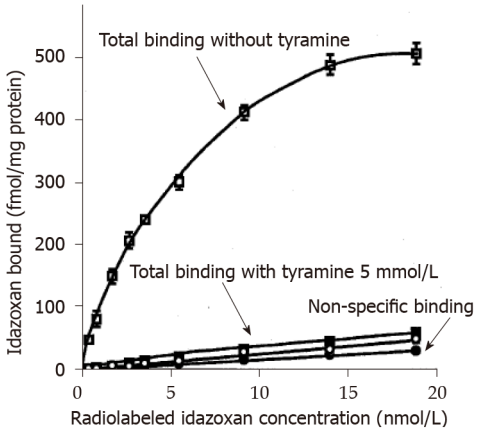

Figure 8 Influence of tyramine on idazoxan binding to liver crude membranes. Total and non-specific binding of ^{3}H-idazoxan to liver crude membranes from lean Zucker rats is shown without (open symbols) and with 5 mmol/L tyramine (closed symbols) added prior to 45-min incubation at room temperature. Without tyramine, the resulting specific binding was characterized by a B_{max} of 622 ± 15 fmol/mg protein and a K_D of 5.1 ± 0.4 nmol/L. Each point is the mean ± SEM of three liver preparations containing 617 ± 120 μg protein/assay. Inhibitory influence of tyramine on total binding was significant at $P < 0.001$.

Thus, the effects of *in vivo* tyramine + vanadate treatment could not reveal relevant antidiabetic or anti-obesity properties, at least at the dose and duration tested. However, the limited - but encouraging - beneficial influence of this treatment on hyperglycemia and hypertriglyceridemia leaves opens the possibility to improve metabolic control by providing MAO substrates, which might enhance glucose

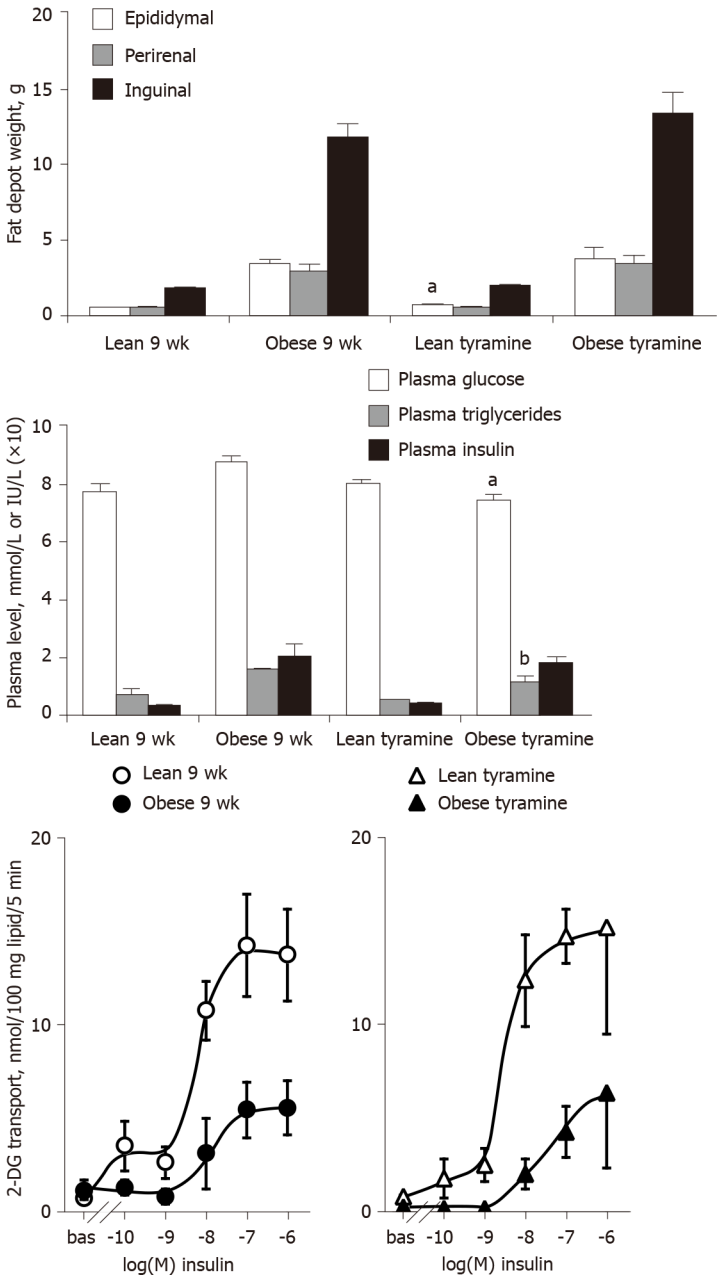

Figure 9 Influence of 'tyramine + vanadate' treatment on adiposity, glucose and lipid handling, and insulin responsiveness of adipocytes in lean and obese rats. Upper part: Weight of three white adipose tissues from 9-wk old Zucker male rats, either from the lean and obese control groups (left) or from the groups receiving daily s.c. administration of 3 mg/kg tyramine + 0.3 mg/kg vanadate (tyramine, right) for 7 d. Middle part: Glucose, triacylglycerol, and insulin fasting plasma levels in the same control and treated groups. Lower part: Hexose transport in adipocytes from lean (open symbols) or obese (closed symbols) rats, in the absence (bas = basal) or presence of the indicated doses of insulin in control (circles) or treated (triangles) groups. Each column or point is the mean ± SEM of three treated or four control rats per genotype. The influence of genotype on all parameters was identical to that specified in previous figures and not indicated for the sake of clarity. Significant difference between tyramine-treated and corresponding control at: $^{a}P < 0.05$; $^{b}P < 0.01$.

utilization in fat depots and facilitate glucose handling at the expense of a slightly larger fattening.

DISCUSSION

The first unexpected observation of this comparison between obese and lean Zucker rats was that the stimulatory effect of millimolar dose of tyramine + vanadate on glucose uptake in adipocytes was altered as much as that of insulin in the obese rat.

Obviously, insulin resistance of adipocytes from obese Zucker rat was expected, and fully confirmed here, but it could be supposed that agents that act independently from insulin receptor activation were less hampered with obesity.

Indeed, many factors could be involved in the decreased insulin-like effect of the combination tyramine + vanadate or benzylamine + vanadate on adipocytes from obese rats, such as altered glucose transporter equipment and recruitment[41]. Anyhow, our initial working hypothesis was based on a putative reduction in the amount of adipose amine oxidases since we recently reported that mice bearing genetic invalidations of SSAO are obese[31].

The second major finding was that, contrarily to our assumptions, MAO activity was higher in the WAT of obese rats than in lean ones. In other words, the MAO substrate tyramine was not more efficient in activating glucose utilization while its degradation was increased in adipocytes from obese animals. This could have a sense if tyramine effect was mediated by a receptor-dependent mechanism, thereby considering that its increased degradation hampered receptor activation. But, in the case of tyramine, the insulin-like effect on glucose utilization by rat adipocytes is mediated by amine oxidation and subsequent hydrogen peroxide release[34]. This is also the case for various other amine oxidase substrates, such as benzylamine or methylamine, which are also active in rodent[42] and human adipocytes[43].

Although the insulin-mimicking action of tyramine is tremendously potentiated by vanadium[34], it was amazing to observe a decrease of such MAO-mediated response together with an increase of MAO activity in the adipocytes from obese rats. We confirmed the latter increase with regard to the level of enzyme activity, protein immunoreactivity, and an increased number of I_2 imidazoline binding sites, located on this mitochondrial enzyme[24,25,32]. Unfortunately, we encountered some technical difficulties with the quantification of rat MAO mRNA despite our know-how developed on MAO expression in the mouse WAT[31]. Consequently, we cannot add to the above converging data that the expression of the genes *Maoa* and *Maob* is increased in the WAT of obese Zucker rats. Despite such limitation, our study clearly indicates that the obesity-related increase of MAO activity was selective of WAT and of BAT, since no change was detected in the liver or in skeletal muscle. Moreover, MAO up-regulation was not paralleled by similar changes of SSAO in WAT. This will be discussed below after summarizing other major metabolic and endocrine defects of the obese Zucker rats that have been confirmed in the present study.

The overweight of the obese rats used for this comparative approach, and the stabilization of their fasting blood glucose close to the normal range at the expense of dramatically increased insulin levels are characteristic traits of this obesity model, which were highly similar to those primarily described for over half a century in the Zucker fatty rat[44]. While the original pioneering findings demonstrated the insulin resistance of skeletal muscles from obese Zucker rats, we confirm here the insulin resistance of white adipocytes at the level of glucose transport and lipogenic activities. More importantly, such insulin resistance was associated in WAT to dysregulations not described so far.

Thus, MAO activity, MAO immunoreactive protein amount, and imidazoline I_2-binding site population were increased in adipocytes from the obese Zucker rats. In muscles of the same animals, the low expression of MAO and SSAO, already documented by diverse techniques[45,46], was unmodified in spite of similar insulin resistance regarding glucose utilization[44]. Facing to such tissue-specific difference, it was therefore difficult to establish a mere link between MAO expression and insulin sensitivity. Although the mechanisms underlying the overexpression of MAO activity specifically in WAT and BAT could not be deciphered here, it must be reminded that MAO is regulated in various organs by numerous factors, including aging, and in different directions for A and B forms[27]. This complexity of regulations may explain why the decreased hepatic MAO previously found in obese rats[23] was not confirmed here. Other possible explanation of this discrepancy can be that in the previous study, it was the decreased mitochondrial content per mass of fatty liver that was the drive for the observed reduction, while in the present study MAO activity was expressed per mass unit of crude membrane proteins. In WAT and BAT, whether adipose MAO was up-regulated by an excess of its substrates as a consequence of the hyperphagia driving obesity remains speculative, and has no rationale to be different from the contradictory changes found in the liver.

Closely related to the MAO increase found in the adipose tissue of obese rats was the increase in imidazoline I_2 binding sites. It occurred only in WAT and was readily visualized by a larger B_{max} for either ^{3}H-BFI or ^{3}H-idazoxan regardless of fat depot anatomical location. The link between I_2 sites and MAO was further supported in the liver by two observations. First, a lack of change between lean and obese rats was found for both parameters: Neither MAO V_{max} nor ^{3}H-BFI B_{max} was altered with obesity in the liver. Second, the ^{3}H-idazoxan binding to hepatic I_2 sites was completely prevented by a high dose of tyramine. These observations complete our previous

report about the capacity of BFI to inhibit MAO-A and MAO-B activities[30]. The obesity-related changes in imidazoline I_2 binding sites seemed to be specific of adipose cells, since no change was evidenced in several other peripheral tissues (this study), and in the brain of obese rats when compared to lean controls[47].

Also of interest was that a lower SSAO activity was concomitant to a larger MAO richness in the adipose cells from obese rats. It can be hypothesized that the small reduction in SSAO activity was involved in the resulting weak insulin-like effect of tyramine, since tyramine is a substrate of both enzymes, at least in rats[34]. Thus, according to our working assumptions, SSAO was reduced in WAT from obese rats, and accordingly the activation of glucose uptake by the SSAO substrate benzylamine (plus vanadate) was diminished.

Indeed, reduced expression of SSAO has been already reported at the level of mRNA abundance and of benzylamine oxidation in the WAT of obese rats as compared with their lean littermates[48]. In this study, the SSAO activity found in the WAT of obese rats was one-half lower than that found in lean controls. Although this reduction is apparently greater than that reported here for immunoreactive SSAO, both observations remain in good agreement. Since benzylamine oxidation was measured *via* a fluorometric method quantifying the hydrogen peroxide production in the previous study[48], it can be supposed *a posteriori* that this had generated underestimates of SSAO activity in obese rats, in view of the increased catalase activity found in their WAT[49]. Such increased catalase might also impair the hydrogen peroxide-dependent activation of glucose uptake that we report here in the obese adipocytes. Whether the decreased SSAO activity in obese WAT is related to a previously reported increase in the spermine and spermidine content of the adipocytes of obese Zucker rats [50] remains to be established, but it must be noted that, alongside their role of regulator of triacylglycerol synthetic enzymes, polyamines are also SSAO substrates. More surely, it can be asserted that the SSAO decrease appeared to be tissue-specific for WAT, as no change in SSAO activity has been found in other anatomical locations (this study), as well as in the aorta of obese Zucker rats[51]. Anyhow, a similar diminution of SSAO has not been found in other animal models of obesity, since modest increases in SSAO activity have been observed in the adipose tissue from db/db mice and dogs fed a high-fat diet when compared to respective control (reviewed in[43]).

It becomes evident that it is not only overweight and WAT hypertrophy that can be related to SSAO expression, but also the overall alteration of glucose and lipid handling of obese states. Of course, SSAO is one of the most abundant proteins present on the cell surface of the adipocytes[52]. SSAO-mediated oxidation of exogenous substrates induces glucose uptake in adipocytes isolated from WAT or obtained by *in vitro* differentiation of preadipose cell lines (reviewed in[43]) and in several other models[53]. SSAO-mediated deamination reactions generate hydrogen peroxide, which also induces antilipolytic and lipogenic effects[54], especially in the presence of vanadate, by forming pervanadate, a potent insulin-like agent[38,55]. More recently, it has been proposed that SSAO interplays with Zinc-α2-glycoprotein[56] and with lipid metabolism in adipocytes[57]. In addition, SSAO is identical to vascular adhesion protein-1 (VAP-1), which supports leukocyte extravasation[58]. These multifunctional facets of SSAO are therefore rendering highly probable the occurrence of various apparently contrasting regulations according to the pathological states of adipose tissues.

Two very recent findings are dealing with our observations of a parallel increase of MAO and I_2 sites in the WAT of obese Zucker rats.

On the one hand, untargeted metabolomics analysis performed in the blood of Zucker diabetic rats indicates that the tryptophan and tyrosine metabolisms are the most dysregulated pathways in this model[59]. This is somewhat dealing with our description of changes in MAO activity occurring in the insulin-resistant adipocytes from obese rats. First, tryptophan is linked with kynurenine and serotonin, which is readily oxidized by MAO and generates 5-hydroxyindoleacetic acid. Second, tyrosine is the precursor of biosynthetic pathways for catecholamines and trace amines and therefore an important source of MAO substrates. By associating these two independent findings, it can be assumed that both biosynthesis and degradation of catecholamines are altered in the obese Zucker rat. Although poorly described, catecholamine catabolism occurs in adipose tissues, especially in visceral WAT, and has been shown to influence both glucose metabolism[60] and adrenergic contraction of mesenteric arteries[61].

On the other hand, it has been proposed during the completion of this work that creatine kinase B controls futile creatine cycling, and is powerfully induced by thermogenic stimuli in both mouse and human adipocytes[62]. Intriguingly, creatine

kinase B has also been proposed to be an imidazoline binding protein in rodents[36]. Indeed, "non-MAO" imidazoline binding sites have been evidenced in diverse mammalian tissues, such as those related to brain creatine kinase B[63]. At the present time, one limitation of our study is that we cannot attest that the reported ^{3}H-idazoxan and ^{3}H-BFI B_{max} values are overestimating or not the MAO quantity in the studied peripheral tissues.

Although we have already documented that I_2 site ligands inhibit MAO[24] and in spite of confirming this link in the present study, it is necessary to remind that we have serendipitously described the antilipolytic properties of 0.1-1 mmol/L BFI in human fat cells without bringing clear demonstration of the underlying mechanisms[30]. Whether the "non-MAO" imidazoline binding sites such as creatine kinase B are involved in this effect as well as the obesity-related changes of I_2 sites in WAT remains to be established.

CONCLUSION

This work is reporting for the first time an adipocyte-specific increase of both MAO and I_2 sites in obese Zucker rats when compared to their lean controls. In spite of this higher capacity of catabolizing endogenous or exogenous amines, the insulin-like effects of tyramine and benzylamine, decreased as much as the insulin activation of glucose transport in the large fat cells of the obese rat. It remains to establish whether the activation of glucose uptake by MAO and SSAO substrates, which can be readily observed *in vitro* in the presence of vanadate, really occurs *in vivo* and might help the insulin-resistant fat cells in storing energy under the form of lipids.

ARTICLE HIGHLIGHTS

Research background

The genetically obese Zucker rat is hyperphagic and accumulates the excess of calorie intake in the form of lipids in spite of the insulin-resistant state of its adipocytes.

Research motivation

To investigate what biological events or natural biochemical processes drive the glucose utilization in fat cells of obese Zucker rats, which are not fully responsive to the lipogenic action of insulin.

Research objectives

Hydrogen peroxide is a biological chemical that can mimic several insulin actions on adipocytes, such as stimulating glucose entry and lipogenesis, and inhibiting lipolysis. Since it is a product of various enzymes in adipocytes, we focused our objective in searching whether the expression activity and biological effect of two types of them, namely, the monoamine oxidase (MAO) and semicarbazide sensitive amine oxidase (SSAO), abundant in adipocytes, were modified in obesity states.

Research methods

Experimental methods included Zucker rat husbandry, with obese and lean littermates (the former bearing homozygotous recessive mutation of fa/fa gene), preparations of freshly isolated adipocytes, functional exploration of hexose transport using uptake assays with appropriate pharmacological agents, and determination of lipogenic activity, immunobloting, measurement of amine oxidase activities, and saturation binding analyses.

Research results

There is a good relationship between the increased binding capacity of tritiated-idazoxan and tritiated-(2-benzofuranyl)-2-imidazoline to imidazoline binding sites and the increased MAO-dependent tyramine oxidation in adipose tissue of obese rats. Stimulation of MAO or SSAO by their substrates in the presence of vanadate reproduced approximately two-thirds of the insulin stimulation of glucose uptake in fat cells. However, this insulin-like effect decreased as the insulin responsiveness of adipocytes decreased with obesity.

Research conclusions

It cannot be stated whether the changes in MAO and SSAO expression are a cause or a consequence of the altered glucose handling in the fat cells of obese Zucker rats. At least, the increased tyramine oxidation is found in adipose tissues of the obese rats, not in the liver or in skeletal muscles, and can be associated with the dysregulation of the catecholaminergic system and of the energy balance found in that animal model of genetic obesity.

Research perspectives

The increase of MAO activity in adipose tissue from obese rats has never been reported, at least to our knowledge. Among the limitations of our first description of an increased MAO activity in the adipose tissue of this animal model of obesity, is that we did not decipher the mechanisms supporting such up-regulation, and that it remains unclear whether elevated MAO is a cause or a consequence of the dysmetabolic profile of the Zucker obese rats. This issue deserves further investigations.

ACKNOWLEDGEMENTS

We thank the staff of animal unit CREFRE, headed by Dr. Collet X (Toulouse, France) and Dr. Guerre-Millo M (Paris, France), for their knowledge about Zucker rat physiology. The authors are also indebted for the invaluable technical assistance of Pré vot D & Jousseaume M, and for the hierarchical benevolence of Bouloumié A.

REFERENCES

1 **Zucker LM**, Zucker TF. Fatty, a new mutation in the rat. *J Heredity* 1961; **52**: 275-278
2 **Chua SC Jr**, Chung WK, Wu-Peng XS, Zhang Y, Liu SM, Tartaglia L, Leibel RL. Phenotypes of mouse diabetes and rat fatty due to mutations in the OB (leptin) receptor. *Science* 1996; **271**: 994-996 [PMID: 8584938 DOI: 10.1126/science.271.5251.994]
3 **Phillips MS**, Liu Q, Hammond HA, Dugan V, Hey PJ, Caskey CJ, Hess JF. Leptin receptor missense mutation in the fatty Zucker rat. *Nat Genet* 1996; **13**: 18-19 [PMID: 8673096 DOI: 10.1038/ng0596-18]
4 **Takaya K**, Ogawa Y, Isse N, Okazaki T, Satoh N, Masuzaki H, Mori K, Tamura N, Hosoda K, Nakao K. Molecular cloning of rat leptin receptor isoform complementary DNAs--identification of a missense mutation in Zucker fatty (fa/fa) rats. *Biochem Biophys Res Commun* 1996; **225**: 75-83 [PMID: 8769097 DOI: 10.1006/bbrc.1996.1133]
5 **Himms-Hagen J**. Physiological roles of the leptin endocrine system: differences between mice and humans. *Crit Rev Clin Lab Sci* 1999; **36**: 575-655 [PMID: 10656540 DOI: 10.1080/10408369991239259]
6 **Michel O**, Heudes D, Lamarre I, Masurier C, Lavau M, Bariety J, Chevalier J. Reduction of insulin and triglycerides delays glomerulosclerosis in obese Zucker rats. *Kidney Int* 1997; **52**: 1532-1542 [PMID: 9407498 DOI: 10.1038/ki.1997.483]
7 **Debant A**, Guerre-Millo M, Le Marchand-Brustel Y, Freychet P, Lavau M, Van Obberghen E. Insulin receptor kinase is hyperresponsive in adipocytes of young obese Zucker rats. *Am J Physiol* 1987; **252**: E273-E278 [PMID: 3548422 DOI: 10.1152/ajpendo.1987.252.2.E273]
8 **Bazin R**, Lavau M. Development of hepatic and adipose tissue lipogenic enzymes and insulinemia during suckling and weaning on to a high-fat diet in Zucker rats. *J Lipid Res* 1982; **23**: 839-849 [PMID: 6752318]
9 **Johnson PR**, Zucker LM, Cruce JA, Hirsch J. Cellularity of adipose depots in the genetically obese Zucker rat. *J Lipid Res* 1971; **12**: 706-714 [PMID: 5124535]
10 **Stern JS**, Johnson PR, Batchelor BR, Zucker LM, Hirsch J. Pancreatic insulin release and peripheral tissue resistance in Zucker obese rats fed high- and low-carbohydrate diets. *Am J Physiol* 1975; **228**: 543-548 [PMID: 1091158 DOI: 10.1152/ajplegacy.1975.228.2.543]
11 **Hardie LJ**, Rayner DV, Holmes S, Trayhurn P. Circulating leptin levels are modulated by fasting, cold exposure and insulin administration in lean but not Zucker (fa/fa) rats as measured by ELISA. *Biochem Biophys Res Commun* 1996; **223**: 660-665 [PMID: 8687452 DOI: 10.1006/bbrc.1996.0951]
12 **Jacob S**, Fogt DL, Dietze GJ, Henriksen EJ. The beta2-adrenergic modulator celiprolol reduces insulin resistance in obese Zucker rats. *Life Sci* 1999; **64**: 2071-2079 [PMID: 10374932 DOI: 10.1016/s0024-3205(99)00154-x]
13 **Pan SJ**, Hancock J, Ding Z, Fogt D, Lee M, Ivy JL. Effects of clenbuterol on insulin resistance in conscious obese Zucker rats. *Am J Physiol Endocrinol Metab* 2001; **280**: E554-E561 [PMID: 11254461 DOI: 10.1152/ajpendo.2001.280.4.E554]
14 **Rothwell NJ**, Stock MJ. Influence of clenbuterol on energy balance, thermogenesis and body composition in lean and genetically obese Zucker rats. *Int J Obes* 1987; **11**: 641-647 [PMID:

3440683]
15 **Mory G**, Wiel M, Adli H, Diot-Dupuy F, Ferré P, Bazin R. Impaired beta-adrenergic signaling pathway in white adipocytes of suckling fa/fa Zucker rats: a defect in receptor coupling. *Int J Obes Relat Metab Disord* 2001; **25**: 1592-1598 [PMID: 11753576 DOI: 10.1038/sj.ijo.0801811]
16 **Lent-Schochet D**, McLaughlin M, Ramakrishnan N, Jialal I. Exploratory metabolomics of metabolic syndrome: A status report. *World J Diabetes* 2019; **10**: 23-36 [PMID: 30697368 DOI: 10.4239/wjd.v10.i1.23]
17 **Bairras C**, Mauriege P, Bukowiecki L, Atgie C. Regulation of lypolysis in white adipose tissues of lean and obese Zucker rats. *J Physiol Biochem* 2007; **63**: 287-296 [PMID: 18457004 DOI: 10.1007/bf03165760]
18 **Mukaida S**, Evans BA, Bengtsson T, Hutchinson DS, Sato M. Adrenoceptors promote glucose uptake into adipocytes and muscle by an insulin-independent signaling pathway involving mechanistic target of rapamycin complex 2. *Pharmacol Res* 2017; **116**: 87-92 [PMID: 28025104 DOI: 10.1016/j.phrs.2016.12.022]
19 **Chernogubova E**, Cannon B, Bengtsson T. Norepinephrine increases glucose transport in brown adipocytes *via* beta3-adrenoceptors through a cAMP, PKA, and PI3-kinase-dependent pathway stimulating conventional and novel PKCs. *Endocrinology* 2004; **145**: 269-280 [PMID: 14551227 DOI: 10.1210/en.2003-0857]
20 **Fontaine J**, Tavernier G, Morin N, Carpéné C. Vanadium-dependent activation of glucose transport in adipocytes by catecholamines is not mediated *via* adrenoceptor stimulation or monoamine oxidase activity. *World J Diabetes* 2020; **11**: 622-643 [PMID: 33384769 DOI: 10.4239/wjd.v11.i12.622]
21 **Nguyen KD**, Qiu Y, Cui X, Goh YP, Mwangi J, David T, Mukundan L, Brombacher F, Locksley RM, Chawla A. Alternatively activated macrophages produce catecholamines to sustain adaptive thermogenesis. *Nature* 2011; **480**: 104-108 [PMID: 22101429 DOI: 10.1038/nature10653]
22 **Fischer K**, Ruiz HH, Jhun K, Finan B, Oberlin DJ, van der Heide V, Kalinovich AV, Petrovic N, Wolf Y, Clemmensen C, Shin AC, Divanovic S, Brombacher F, Glasmacher E, Keipert S, Jastroch M, Nagler J, Schramm KW, Medrikova D, Collden G, Woods SC, Herzig S, Homann D, Jung S, Nedergaard J, Cannon B, Tschöp MH, Müller TD, Buettner C. Alternatively activated macrophages do not synthesize catecholamines or contribute to adipose tissue adaptive thermogenesis. *Nat Med* 2017; **23**: 623-630 [PMID: 28414329 DOI: 10.1038/nm.4316]
23 **Clouet P**, Henninger C, Bézard J. Study of some factors controlling fatty acid oxidation in liver mitochondria of obese Zucker rats. *Biochem J* 1986; **239**: 103-108 [PMID: 3800970 DOI: 10.1042/bj2390103]
24 **Carpéné C**, Collon P, Remaury A, Cordi A, Hudson A, Nutt D, Lafontan M. Inhibition of amine oxidase activity by derivatives that recognize imidazoline I2 sites. *J Pharmacol Exp Ther* 1995; **272**: 681-688 [PMID: 7853182]
25 **Limon-Boulez I**, Tesson F, Gargalidis-Moudanos C, Parini A. I2-imidazoline binding sites: relationship with different monoamine oxidase domains and identification of histidine residues mediating ligand binding regulation by H+1. *J Pharmacol Exp Ther* 1996; **276**: 359-364 [PMID: 8632297]
26 **Basile L**, Pappalardo M, Guccione S, Milardi D, Ramsay RR. Computational comparison of imidazoline association with the I2 binding site in human monoamine oxidases. *J Chem Inf Model* 2014; **54**: 1200-1207 [PMID: 24601544 DOI: 10.1021/ci400346k]
27 **Tipton KF**. 90 years of monoamine oxidase: some progress and some confusion. *J Neural Transm (Vienna)* 2018; **125**: 1519-1551 [PMID: 29637260 DOI: 10.1007/s00702-018-1881-5]
28 **Kilkenny C**, Browne W, Cuthill IC, Emerson M, Altman DG; NC3Rs Reporting Guidelines Working Group. Animal research: reporting in vivo experiments: the ARRIVE guidelines. *Br J Pharmacol* 2010; **160**: 1577-1579 [PMID: 20649561 DOI: 10.1111/j.1476-5381.2010.00872.x.]
29 **Moody AJ**, Stan MA, Stan M, Gliemann J. A simple free fat cell bioassay for insulin. *Horm Metab Res* 1974; **6**: 12-16 [PMID: 4819286 DOI: 10.1055/s-0028-1093895]
30 **Bour S**, Iglesias-Osma MC, Marti L, Duro P, Garcia-Barrado MJ, Pastor MF, Prévot D, Visentin V, Valet P, Moratinos J, Carpéné C. The imidazoline I2-site ligands BU 224 and 2-BFI inhibit MAO-A and MAO-B activities, hydrogen peroxide production, and lipolysis in rodent and human adipocytes. *Eur J Pharmacol* 2006; **552**: 20-30 [PMID: 17056035 DOI: 10.1016/j.ejphar.2006.09.021]
31 **Jargaud V**, Bour S, Tercé F, Collet X, Valet P, Bouloumié A, Guillemot JC, Mauriège P, Jalkanen S, Stolen C, Salmi M, Smith DJ, Carpéné C. Obesity of mice lacking VAP-1/SSAO by Aoc3 gene deletion is reproduced in mice expressing a mutated vascular adhesion protein-1 (VAP-1) devoid of amine oxidase activity. *J Physiol Biochem* 2021; 77: 141-154 [PMID: 32712883 DOI: 10.1007/s13105-020-00756-y]
32 **Remaury A**, Raddatz R, Ordener C, Savic S, Shih JC, Chen K, Seif I, De Maeyer E, Lanier SM, Parini A. Analysis of the pharmacological and molecular heterogeneity of I(2)-imidazoline-binding proteins using monoamine oxidase-deficient mouse models. *Mol Pharmacol* 2000; **58**: 1085-1090 [PMID: 11040057 DOI: 10.1124/mol.58.5.1085]
33 **Ramonet D**, Rodríguez M, Saura J, Lizcano JM, Romera M, Unzeta M, Finch C, Billett E, Mahy N. Localization of monoamine oxidase A and B and semicarbazide-sensitive amine oxidase in human peripheral tissues. *Inflammopharmacology* 2003; **11**: 111-117 [PMID: 15035812 DOI: 10.1163/156856003765764272]
34 **Marti L**, Morin N, Enrique-Tarancon G, Prevot D, Lafontan M, Testar X, Zorzano A, Carpéné C. Tyramine and vanadate synergistically stimulate glucose transport in rat adipocytes by amine oxidase-

dependent generation of hydrogen peroxide. *J Pharmacol Exp Ther* 1998; **285**: 342-349 [PMID: 9536030]

35 **Miralles A**, Esteban S, Sastre-Coll A, Moranta D, Asensio VJ, García-Sevilla JA. High-affinity binding of beta-carbolines to imidazoline I2B receptors and MAO-A in rat tissues: norharman blocks the effect of morphine withdrawal on DOPA/noradrenaline synthesis in the brain. *Eur J Pharmacol* 2005; **518**: 234-242 [PMID: 16061219 DOI: 10.1016/j.ejphar.2005.06.023]

36 **Kimura A**, Tyacke RJ, Robinson JJ, Husbands SM, Minchin MC, Nutt DJ, Hudson AL. Identification of an imidazoline binding protein: creatine kinase and an imidazoline-2 binding site. *Brain Res* 2009; **1279**: 21-28 [PMID: 19410564 DOI: 10.1016/j.brainres.2009.04.044]

37 **Lönnroth P**, Eriksson JW, Posner BI, Smith U. Peroxovanadate but not vanadate exerts insulin-like effects in human adipocytes. *Diabetologia* 1993; **36**: 113-116 [PMID: 8458524 DOI: 10.1007/bf00400690]

38 **Aureliano M**. Recent perspectives into biochemistry of decavanadate. *World J Biol Chem* 2011; **2**: 215-225 [PMID: 22031844 DOI: 10.4331/wjbc.v2.i10.215]

39 **Velliquette RA**, Kossover R, Previs SF, Ernsberger P. Lipid-lowering actions of imidazoline antihypertensive agents in metabolic syndrome X. *Naunyn Schmiedebergs Arch Pharmacol* 2006; **372**: 300-312 [PMID: 16416266 DOI: 10.1007/s00210-005-0024-3]

40 **Aubertin G**, Weiss M, Traversi F, Benameur D, Choquet P, Dali-Youcef N, Pons F, Sigrist S, Greney H, Monassier L, Bousquet P, Niederhoffer N. Effects of imidazoline-like drugs on liver and adipose tissues, and their role in preventing obesity and associated cardio-metabolic disorders. *Int J Obes (Lond)* 2019; **43**: 2163-2175 [PMID: 30926950 DOI: 10.1038/s41366-019-0342-z]

41 **Wang T**, Wang J, Hu X, Huang XJ, Chen GX. Current understanding of glucose transporter 4 expression and functional mechanisms. *World J Biol Chem* 2020; **11**: 76-98 [PMID: 33274014 DOI: 10.4331/wjbc.v11.i3.76]

42 **Yu PH**, Wang M, Fan H, Deng Y, Gubisne-Haberle D. Involvement of SSAO-mediated deamination in adipose glucose transport and weight gain in obese diabetic KKAy mice. *Am J Physiol Endocrinol Metab* 2004; **286**: E634-E641 [PMID: 14656718 DOI: 10.1152/ajpendo.00272.2003]

43 **Carpéné C**, Boulet N, Chaplin A, Mercader J. Past, Present and Future Anti-Obesity Effects of Flavin-Containing and/or Copper-Containing Amine Oxidase Inhibitors. *Medicines (Basel)* 2019; **6** [PMID: 30650583 DOI: 10.3390/medicines6010009]

44 **Crettaz M**, Prentki M, Zaninetti D, Jeanrenaud B. Insulin resistance in soleus muscle from obese Zucker rats. Involvement of several defective sites. *Biochem J* 1980; **186**: 525-534 [PMID: 6990920 DOI: 10.1042/bj1860525]

45 **Saura J**, Kettler R, Da Prada M, Richards JG. Quantitative enzyme radioautography with 3H-Ro 41-1049 and 3H-Ro 19-6327 in vitro: localization and abundance of MAO-A and MAO-B in rat CNS, peripheral organs, and human brain. *J Neurosci* 1992; **12**: 1977-1999 [PMID: 1578281 DOI: 10.1523/jneurosci.12-05-01977.1992]

46 **Lewinsohn R**, Böhm K, Glover V, Sandler M. A benzylamine oxidase distinct from monoamine oxidase B--widespread distribution in man and rat. *Biochem Pharmacol* 1978; **27**: 1857-1863 [PMID: 708467 DOI: 10.1016/0006-2952(78)90033-3]

47 **Miralles A**, Ribas C, Olmos G, García-Sevilla JA. No effect of genetic obesity and mazindol on imidazoline I2 binding sites in the brain of Zucker rats. *Eur J Pharmacol* 1993; **243**: 305-308 [PMID: 8276084 DOI: 10.1016/0014-2999(93)90191-j]

48 **Moldes M**, Fève B, Pairault J. Molecular cloning of a major mRNA species in murine 3T3 adipocyte lineage. differentiation-dependent expression, regulation, and identification as semicarbazide-sensitive amine oxidase. *J Biol Chem* 1999; **274**: 9515-9523 [PMID: 10092636 DOI: 10.1074/jbc.274.14.9515]

49 **Galinier A**, Carrière A, Fernandez Y, Carpéné C, André M, Caspar-Bauguil S, Thouvenot JP, Périquet B, Pénicaud L, Casteilla L. Adipose tissue proadipogenic redox changes in obesity. *J Biol Chem* 2006; **281**: 12682-12687 [PMID: 16377639 DOI: 10.1074/jbc.M506949200]

50 **Jamdar SC**, Cao WF, Samaniego E. Relationship between adipose polyamine concentrations and triacylglycerol synthetic enzymes in lean and obese Zucker rats. *Enzyme Protein* 1996; **49**: 222-230 [PMID: 9030889 DOI: 10.1159/000468632]

51 **Liu J**, Wang R, Desai K, Wu L. Upregulation of aldolase B and overproduction of methylglyoxal in vascular tissues from rats with metabolic syndrome. *Cardiovasc Res* 2011; **92**: 494-503 [PMID: 21890532 DOI: 10.1093/cvr/cvr239]

52 **Morris NJ**, Ducret A, Aebersold R, Ross SA, Keller SR, Lienhard GE. Membrane amine oxidase cloning and identification as a major protein in the adipocyte plasma membrane. *J Biol Chem* 1997; **272**: 9388-9392 [PMID: 9083076 DOI: 10.1074/jbc.272.14.9388]

53 **El Hadri K**, Moldes M, Mercier N, Andreani M, Pairault J, Feve B. Semicarbazide-sensitive amine oxidase in vascular smooth muscle cells: differentiation-dependent expression and role in glucose uptake. *Arterioscler Thromb Vasc Biol* 2002; **22**: 89-94 [PMID: 11788466 DOI: 10.1161/hq0102.101550]

54 **Mukherjee SP**. Mediation of the antilipolytic and lipogenic effects of insulin in adipocytes by intracellular accumulation of hydrogen peroxide. *Biochem Pharmacol* 1980; **29**: 1239-1246 [PMID: 6249328 DOI: 10.1016/0006-2952(80)90280-4]

55 **Shisheva A**, Shechter Y. Mechanism of pervanadate stimulation and potentiation of insulin-activated glucose transport in rat adipocytes: dissociation from vanadate effect. *Endocrinology* 1993; **133**: 1562-1568 [PMID: 8404595 DOI: 10.1210/endo.133.4.8404595]

56 **Romauch M**. Zinc-α2-glycoprotein as an inhibitor of amine oxidase copper-containing 3. *Open Biol* 2020; **10**: 190035 [PMID: 32315567 DOI: 10.1098/rsob.190035]

57 **Yang H**, Ralle M, Wolfgang MJ, Dhawan N, Burkhead JL, Rodriguez S, Kaplan JH, Wong GW, Haughey N, Lutsenko S. Copper-dependent amino oxidase 3 governs selection of metabolic fuels in adipocytes. *PLoS Biol* 2018; **16**: e2006519 [PMID: 30199530 DOI: 10.1371/journal.pbio.2006519]

58 **Salmi M**, Jalkanen S. Vascular Adhesion Protein-1: A Cell Surface Amine Oxidase in Translation. *Antioxid Redox Signal* 2019; **30**: 314-332 [PMID: 29065711 DOI: 10.1089/ars.2017.7418]

59 **Liu Q**, Quach SY. Untargeted metabolomics analysis of serum metabolites in Zucker diabetic fatty rats. *E3S Web of Conferences* 2021; **233**: 02017 [DOI: 10.1051/e3sconf/202123302017]

60 **Walton RG**, Zhu X, Tian L, Heywood EB, Liu J, Hill HS, Bruemmer D, Yang Q, Fu Y, Garvey WT. AP2-NR4A3 transgenic mice display reduced serum epinephrine because of increased catecholamine catabolism in adipose tissue. *Am J Physiol Endocrinol Metab* 2016; **311**: E69-E81 [PMID: 27166283 DOI: 10.1152/ajpendo.00330.2015]

61 **Ayala-Lopez N**, Thompson JM, Watts SW. Perivascular Adipose Tissue's Impact on Norepinephrine-Induced Contraction of Mesenteric Resistance Arteries. *Front Physiol* 2017; **8**: 37 [PMID: 28228728 DOI: 10.3389/fphys.2017.00037]

62 **Rahbani JF**, Roesler A, Hussain MF, Samborska B, Dykstra CB, Tsai L, Jedrychowski MP, Vergnes L, Reue K, Spiegelman BM, Kazak L. Creatine kinase B controls futile creatine cycling in thermogenic fat. *Nature* 2021; **590**: 480-485 [PMID: 33597756 DOI: 10.1038/s41586-021-03221-y]

63 **Li JX**. Imidazoline I_2 receptors: An update. *Pharmacol Ther* 2017; **178**: 48-56 [PMID: 28322973 DOI: 10.1016/j.pharmthera.2017.03.009]

Published by **Baishideng Publishing Group Inc**
7041 Koll Center Parkway, Suite 160, Pleasanton, CA 94566, USA
Telephone: +1-925-3991568
E-mail: bpgoffice@wjgnet.com
Help Desk: https://www.f6publishing.com/helpdesk
https://www.wjgnet.com